



120  
301  
THS

AN INVESTIGATION OF DYNAMIC STRESSES IN  
A CAM FOLLOWER SYSTEM USING AN  
ELECTRONIC DIFFERENTIAL ANALYZER

Thesis for the Degree of M. S.  
MICHIGAN STATE UNIVERSITY  
Armando Louis Odorico  
1958



This is to certify that the

thesis entitled

AN INVESTIGATION OF DYNAMIC STRESSES IN A CAM FOLLOWER  
SYSTEM USING AN ELECTROMIC DIFFERENTIAL ANALYZER

presented by

ARMANDO L. ODORICO

has been accepted towards fulfillment  
of the requirements for

MASTER OF SCIENCE degree in APPLIED MECHANICS

  
Major professor

Date MAY 21, 1958

**PLACE IN RETURN BOX to remove this checkout from your record.  
TO AVOID FINES return on or before date due.**

DATE DUE DATE DUE DATE DUE		
1170 1196 12-04/8102	_____	_____
_____	_____	_____
_____	_____	_____
_____	_____	_____
_____	_____	_____
_____	_____	_____
_____	_____	_____

**MSU is An Affirmative Action/Equal Opportunity Institution**

c:\circ\dateduea.pr3-p.1



AN INVESTIGATION OF DYNAMIC STRESSES  
IN A CAM FOLLOWER SYSTEM USING AN  
ELECTRONIC DIFFERENTIAL ANALYZER

by

Armando Louis Odorico

AN ABSTRACT

Submitted to the School of Graduate Studies of Michigan  
State University of Agriculture and Applied Science  
in partial fulfillment of the requirements  
for the degree of

MASTER OF SCIENCE

Department of Applied Mechanics

1958

Approved:

Samuel Mercer, Jr.

In this research ten theoretical cam contours were studied. The maximum dynamic stresses of a follower system during a single cam stroke were calculated. The maximum residual stresses in the follower system after the cam stroke were also calculated to check the validity of the results. The specific problem undertaken was to attempt to find a relationship between the dynamic and residual stresses.

A simple spring and mass model was used to represent a typical follower system. The model was considered to have one degree of freedom and was excited by a cam form. A differential equation representing the response of the follower system was developed. The solution of this equation was made on an analog computer and the results were recorded on an oscillograph. By simple operations, these results were transformed into data used to plot the residual stress factor and dynamic stress factor in non-dimensional form.

The dynamic stress factor and residual stress factor curves were determined for the ten cams. A comparison between these two curves was made and a relationship was found to exist. A simple equation was developed by which the maximum dynamic stress could be approximated when the residual stress is known. This equation is of practical value to a designer since it can give results quickly and simply.

AN INVESTIGATION OF DYNAMIC STRESSES  
IN A CAM FOLLOWER SYSTEM USING AN  
ELECTRONIC DIFFERENTIAL ANALYZER

by

Armando Louis Odorico

A THESIS

Submitted to the School of Graduate Studies of Michigan  
State University of Agriculture and Applied Science  
in partial fulfillment of the requirements  
for the degree of

MASTER OF SCIENCE

Department of Applied Mechanics

1958

6-19-55  
65837

#### ACKNOWLEDGMENTS

The author wishes to express his sincere gratitude to Dr. Samuel Mercer, Jr. for the suggestion of the thesis and his invaluable guidance in its preparation.

He is also greatly indebted to the Michigan State University Engineering Experiment Station for the supplies and equipment necessary for performing the research.

Grateful acknowledgment is also due to Clarence Chambers for the photographs included in the thesis.



## TABLE OF CONTENTS

	PAGE
INTRODUCTION. . . . .	1
PREVIOUS INVESTIGATIONS . . . . .	3
SPECIFIC PROBLEM . . . . .	7
THEORY. . . . .	8
Assumptions . . . . .	8
Basic Mathematical Equation. . . . .	8
Equations for Calculating Data. . . . .	10
DESCRIPTION OF EQUIPMENT. . . . .	15
Curves. . . . .	15
Function Generator. . . . .	16
Differential Analyzer. . . . .	17
Sanborn Record . . . . .	17
PROCEDURE. . . . .	19
ACCURACY . . . . .	20
SAMPLE CALCULATIONS . . . . .	21
DISCUSSION OF RESULTS. . . . .	23
Comparison with Published Results. . . . .	23
Residual Stress Factor . . . . .	23
Dynamic Stress Factor. . . . .	25
Relationship Between Curves. . . . .	26
CONCLUSIONS . . . . .	38
POSSIBILITIES FOR FUTURE STUDIES . . . . .	40
BIBLIOGRAPHY. . . . .	41
APPENDIX . . . . .	42

## LIST OF FIGURES

FIGURE		PAGE
1.	Model of Cam and Follower. . . . .	9
2.	Results of Calculations Made on the Differential Analyzer . . . . .	12
3.	Equipment Used to Obtain Results . . . . .	14
4.	Function Generator and Curve. . . . .	15
5.	Differential Analyzer . . . . .	16
6.	Schematic Diagram of Differential Analyzer Circuit. . . . .	18
7.	Dynamic and Residual Stress Characteristics for Seventh Degree Polynomial Cam . . . . .	27
8.	Dynamic and Residual Stress Characteristics for Cam A . . . . .	28
9.	Dynamic and Residual Stress Characteristics for Cam B . . . . .	29
10.	Dynamic and Residual Stress Characteristics for Cam C . . . . .	30
11.	Dynamic and Residual Stress Characteristics for Cam E . . . . .	31
12.	Dynamic and Residual Stress Characteristics for Cam F . . . . .	32
13.	Dynamic and Residual Stress Characteristics for Cam G . . . . .	33
14.	Dynamic and Residual Stress Characteristics for Cam H . . . . .	34
15.	Dynamic and Residual Stress Characteristics for Double Cycloid Cam. . . . .	35

FIGURE	PAGE
16. Dynamic and Residual Stress Characteristics for Triple Cycloid Cam. . . . .	36
17. Dynamic and Residual Stress Characteristics for Triple Cycloid Cam With Empirical Curve. . . . .	37
18. Acceleration Specifications for Cam A. . . . .	42
19. Acceleration Specifications for Cam B. . . . .	42
20. Acceleration Specifications for Cam C. . . . .	43
21. Acceleration Specifications for Cam E. . . . .	43
22. Acceleration Specifications for Cam F. . . . .	44
23. Acceleration Specifications for Cam G. . . . .	44
24. Acceleration Specifications for Cam H. . . . .	45
25. Acceleration Specifications for Cam Polynomial. . . . .	45
26. Acceleration Specifications for Cam Double Cycloid . . . . .	46
27. Acceleration Specifications for Cam Triple Cycloid . . . . .	46

## DEFINITIONS OF SYMBOLS AND TERMS

Z	Absolute displacement of mass	in.
X	Absolute cam displacement	in.
Y	Displacement of mass relative to cam surface	in.
Z,X,Y	Second derivatives of Z, X, Y with respect to time	in./sec. <sup>2</sup>
t	Time	sec.
m	Equivalent mass of system	lb.-sec. <sup>2</sup> /in.
k	Equivalent stiffness of follower system	lb./in.
$\omega_m$	Natural frequency of follower system	rad./sec.
$\omega_c$	Frequency corresponding to cam stroke	rad./sec.
$\tau$	Period of one cycle	sec.
V	Voltage	volts
v	Sanborn Recording Permapaper speed	in./secs.
$L_c$	Chart length corresponding to cam stroke	in.
$L_c$	Chart length corresponding to one cycle of residual vibration	in.
$h_c$	Ordinate of chart corresponding to maximum stress if follower system were rigid	lines
$h_d$	Ordinate of chart corresponding to maximum dynamic stress during cam stroke	lines
$h_n$	Ordinate of chart corresponding to maximum residual stress	lines
f	Number of free vibrations during cam stroke	dimensionless
$C_a$	Maximum acceleration coefficient	dimensionless



- $S_d$  Dynamic stress factor: the ratio of the maximum stress during a cam stroke to the stress that would result if the equivalent mass were accelerated at the maximum cam acceleration multiplied by  $C_a$  dimensionless
- $S_r$  Residual stress factor: the ratio of the maximum residual stress after a single cam stroke to the stress that would result if the equivalent mass were accelerated at the maximum cam acceleration multiplied by  $C_a$  dimensionless

## INTRODUCTION

Cams are extensively used because of their versatility and the ease with which they can be incorporated into systems. A distinct advantage of a cam actuated mechanism is that the desired motion may be changed merely by substituting a different cam form. In many instances, a cam can be substituted for a more complex mechanism and still produce the desired motion. Therefore, cams are used in sewing machines, printing machines, internal combustion engines, and almost all types of automatic machines.

The basic function of a cam is to produce a specified displacement of a follower system. In some applications intermediate points, as well as the initial and final positions, are specified. This narrows the choice of the cam contour. Where the initial and final positions and the time interval between them are the only specifications, a wide choice of cams is available to the designer. The problem of selecting a suitable cam contour arises. A good cam design will be determined on the basis of cost and performance.

When a cam actuated mechanism is operated at a high speed, vibrations result due to the forces exerted on the follower system. By eliminating or reducing the vibrational amplitudes, lower stresses result and cam wear is minimized.

Also, better accuracy can be obtained while operating at higher speeds. Therefore, it is desirable for the designer to have sufficient knowledge of the dynamical response of follower systems.

Some factors that influence follower vibrations are the flexibility of the system, the operating speed, the roughness and waviness of the cam surface, and the theoretical cam contour. No matter how much care is given to other factors, poor dynamic characteristics will result if the theoretical cam contour is not inherently good. Therefore, the choice of a suitable theoretical cam form is of the utmost importance.

This investigation was concerned with the effects of a theoretical cam contour on the vibrational stresses of a follower system. More specifically, the relationship between the maximum stress during a single cam stroke and the maximum residual stress after the cam stroke was studied for ten theoretical cam contours.

## PREVIOUS INVESTIGATIONS

In the past, the conventional cam design procedure was to assume the follower system was composed of rigid bodies. It was not until 1947, when Dudley (2)\* made an investigation of automotive valves, that this assumption no longer seemed valid. The conclusion drawn from Dudley's investigation was that the chief cause of bad valve motion was the flexibility of the follower system.

With this in mind, Dudley used a new approach in cam analysis by considering the flexibility of the follower system. He believed that there were ideal motion curves. These preferred curves were those for which the integral of the acceleration squared was a minimum. Using calculus of variations, the solution obtained was in the form of a polynomial. Therefore, he concluded that the most satisfactory cam form was a polynomial.

In designing a cam, Dudley calculated the inertia forces at the design speed and adjusted the polynomial curve to produce a vibration-free path. This method is called "compensating" a cam. Cam compensating has been widely accepted and proved very successful especially in the automotive industry.

---

\*Numbers in parentheses refer to Bibliography.



In 1944 Hrones (3) made an analysis in which he considered the cam follower system to be an equivalent spring and mass with viscous damping, excited by the cam. In the study, Hrones examined three cam contours: the gravity, harmonic, and cycloidal cams. As a basis for comparison, he used a dimensionless force plot. The gravity and harmonic cams displayed generally inferior stress characteristics compared to those of the cycloidal. This was due to discontinuities in the acceleration curves for the gravity and harmonic cam. The cycloidal acceleration curve had no discontinuities. Hrones also found that as the amount of damping in a system increased, the oscillations about the equilibrium configuration decreased. However, discretion must be used if damping is purposely designed into a system because the peak forces may become very large.

A significant contribution was made in 1950 by Mitchell (7). His experimental study supported the conclusions of Hrones regarding the relative merits of the gravity, harmonic, and cycloidal cams. Although no new conclusions had been reached, the validation of Hrone's results supported the importance of analytical investigations of theoretical cam contours.

Neklutin (8) used two concepts in the analysis of cam follower systems:

1. The shape of the cam should be determined from a selected acceleration diagram, not vice-versa, as was commonly practiced previously.

2. He regarded damping in a follower system to be light and neglected this factor in his analysis.

Further, he maintained that when oscillations persisted, they affected the vibrational amplitudes for subsequent cam strokes. Therefore, Neklutin examined acceleration diagrams and used the residual oscillations as a criterion in his studies. Neklutin plotted his results in the form of dimensionless ratios, the residual stress factor,  $S_r$ , versus the frequency ratio,  $f$ . His results also verified those of Hrones. A significant contribution by Neklutin was his manner of presentation. Where Hrones plotted a curve for all values of time for each frequency ratio, Neklutin plotted a maximum point for each frequency ratio thus obtaining only one curve for each cam contour. Since a designer is usually concerned with the maximum value only, Neklutin's results were compact and concise.

Mercer and Holowenko (5) extended Neklutin's work by using numerical methods to include cam forms that were not amenable to exact mathematical methods. Mercer and Holowenko found it a practical necessity to program the problem for solution on a digital computer. This gave a high degree of accuracy. Another significant contribution was that the residual stress factor curves were related to resonant tendencies for periodic strokes of the cam. An analysis of this type is especially important for cam mechanisms where the output mass is not brought to a positive stop, such as those in indexing machines. Results obtained by Mercer and

100  
100  
100  
100  
100

Holowekno generally substantiated those of Hrones and Neklutin and supported Dudley's theory on the excellence of the polynomial curves.

Studies of the dynamic characteristics of theoretical cam contours have also been made by Anderson (1), Kloomok and Muffley (4), Rothbart (9), and others, but the methods used were similar to those previously mentioned.

## SPECIFIC PROBLEM

As previously mentioned, Neklutin used residual vibrations as an indication of cam excellence. In many mechanisms, such as valve gear in an internal combustion engine, residual vibrations are eliminated because the output mass (valve) is brought to a positive stop. In a mechanism of this type the maximum stress of the follower system is an important design consideration. Since the maximum stress occurs during the cam stroke it is desirable to determine this maximum value. However, determining the stress values during a cam stroke is very tedious, so a more simple method of finding the maximum dynamic stress would be desirable.

The problem undertaken in this thesis was to determine the maximum dynamic stress during a cam stroke and attempt to relate it to the maximum residual stress. A general relationship between the two curves would simplify calculating the dynamic stresses for other cam forms.

## THEORY

### Assumptions

The model of the cam and follower, Figure 1, was selected because it could justifiably represent many cam actuated mechanisms. The characteristics of this model were:

1. The mass of the follower system was represented by a single equivalent mass.
2. The follower was in contact with the cam surface at all times.
3. The stiffness,  $k$ , of the follower system was independent of position.
4. The system had zero damping.
5. The cam was considered to be a rigid body.
6. The cam velocity was constant.

### Basic Mathematical Equation

The method used in arriving at a general differential equation was similar to that of Mercer and Holowenko. The differential equation of motion of the mass,  $m$ , was determined by using Newton's Law,  $F = ma$

$$m\ddot{Z} = -kY \quad [1]$$

Using the relationship from Figure 1

$$Z = X + Y \quad [2]$$

and substituting this into equation [1]

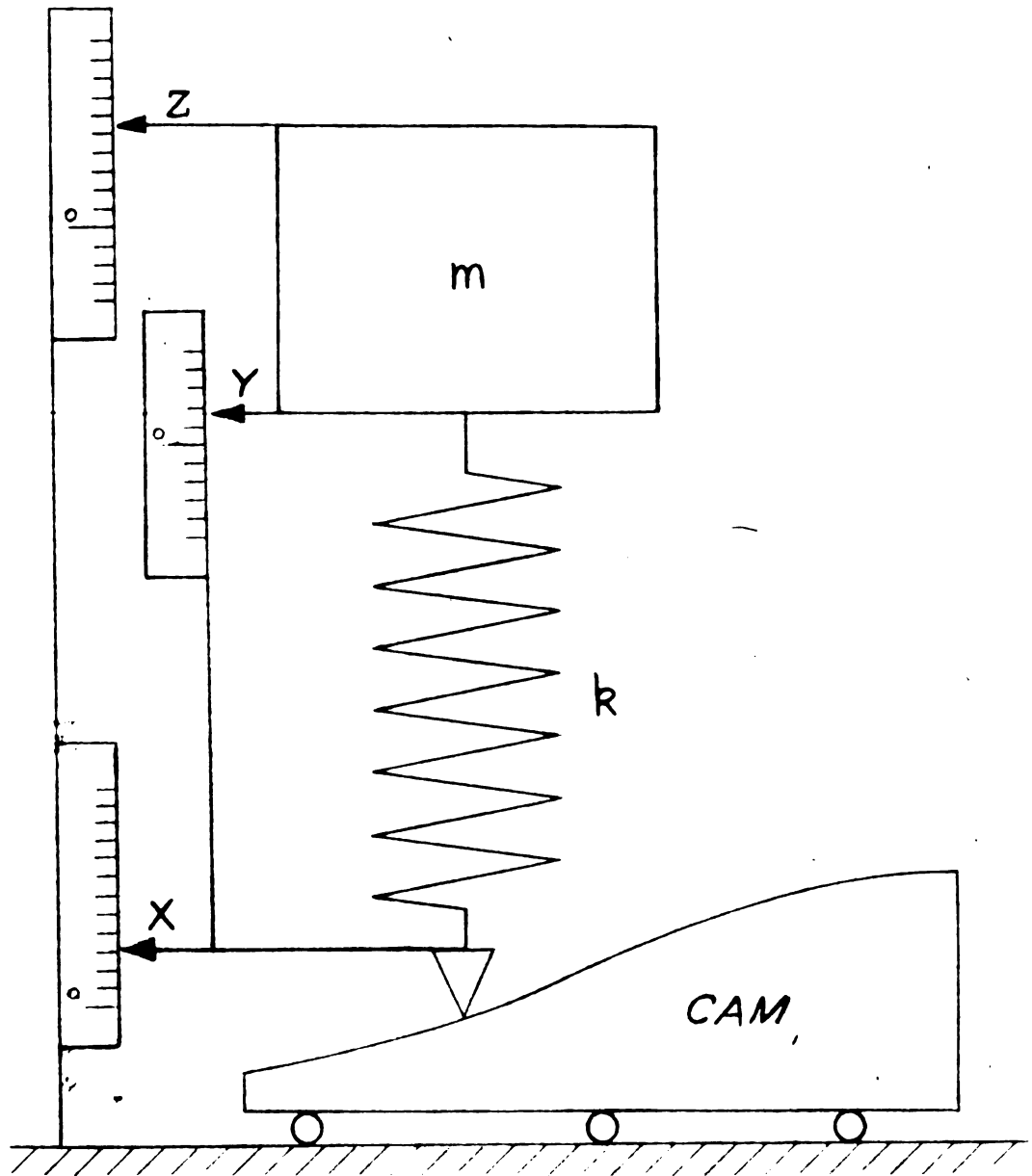


Figure 1. Model of Cam and Follower

$$m(\ddot{X} + \ddot{Y}) = -kY \quad [3]$$

Rearranging and dividing by m

$$\ddot{Y} + \frac{k}{m} Y = -\ddot{X} \quad [4]$$

The solution of equation [4] gave the motion of the follower mass relative to the cam. Three methods of solution were considered. The first method, used by Neklutin, involved the use of Duhamel's integral to get a solution in the form of equation [5].

$$Y(t) = A_t \sin \omega_m t + B_t \cos \omega_m t \quad [5]$$

where

$$\omega_m = \sqrt{\frac{k}{m}} \quad [6]$$

and  $A_t$ ,  $B_t$  are functions of time,  $t$ .

Point solutions for  $Y$  were obtained by solving equation [5] for each desired time,  $t$ .  $A_t$  and  $B_t$  were calculated for each corresponding value of  $t$ . A second method involved expressing the right side of equation [4] as a Fourier expansion, that is, an infinite series of sine and cosine terms. These methods were very tedious. It was found practical to use a third method. This method involved solving equation [3] on an analog computer. The procedure of solution is discussed on page 19.

#### Equations for Calculating Data

It was desirable to compare all cams on an equivalent basis. To do this, each acceleration function was multiplied

by its maximum acceleration coefficient,  $C_a$ . This condition allowed the cams to produce the specified maximum displacement of unity.

The stress factors,  $S_d$  and  $S_r$  were plotted as a function of  $f$ , the number of free vibrations per cam stroke.

By definition

$$f = \frac{\omega_m}{\omega_c} \quad [7]$$

Since the solution of the basic equation [4] was obtained on an oscillograph in the form of a voltage representation, the following equations were developed in order to calculate  $f$ ,  $S_d$ , and  $S_r$ . Refer to Figure 2.

The Sanborn Recording Permapaper speed,  $v$ , was checked and found to be constant. The length of the recording chart corresponding to one cam stroke was

$$L_c = v \tau_c \quad [8]$$

The length of the recording chart corresponding one cycle of residual vibration was

$$L_n = v \tau_n \quad [9]$$

where  $\tau$  is the period of one complete cycle.

Since

$$\omega = \frac{2\pi}{\tau} \quad [10]$$

then

$$\frac{\omega_m}{\omega_c} = \frac{\tau_c}{\tau_m} \quad [11]$$

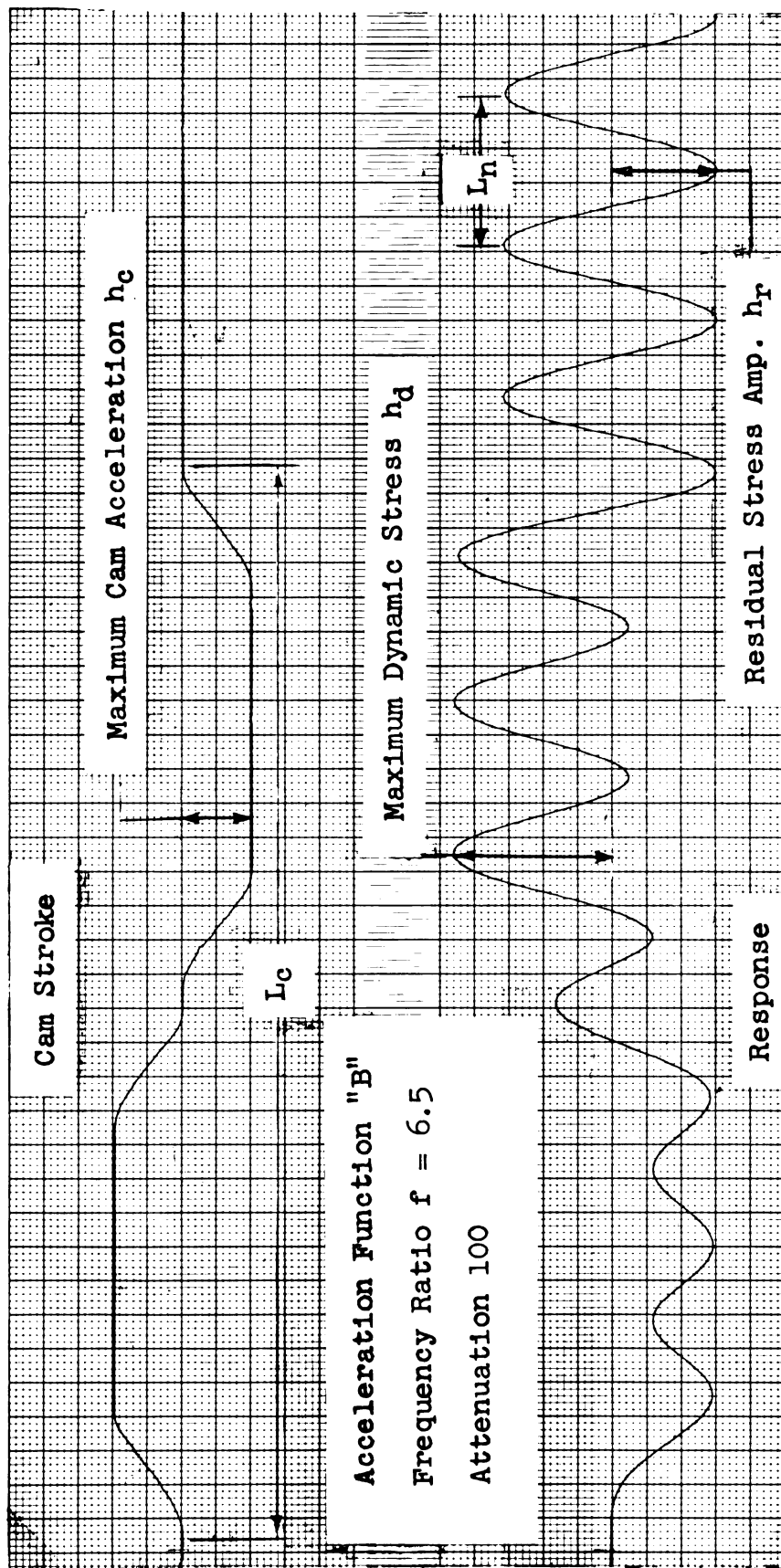


Figure 2. Results of Calculations Made on the Differential Analyzer

From equations [8] and [9]

$$\frac{\tau_c}{\tau_m} = \frac{L_c}{L_m} \quad [12]$$

From equations [7], [11], and [12]

$$f = \frac{\omega_m}{\omega_c} = \frac{L_c}{L_m} \quad [13]$$

The stress factor, S, was defined as

$$S = \frac{F}{F_c} C_a \quad [14]$$

Since the recorded voltage was proportional to the force or stress, then

$$S = \frac{V}{V_c} C_a \quad [15]$$

The oscillograph was calibrated at twenty-five volts for a full scale deflection of twenty-five lines in an attenuation of 100. Therefore,

$$S_d = \frac{\text{Volts/line} \cdot h_d \cdot \text{Att}/100}{\text{Volts/line} \cdot h_c \cdot \text{Att}/100} C_a \quad [16]$$

Similarly

$$S_r = \frac{\text{Volts/line} \cdot h_r \cdot \text{Att}/100}{\text{Volts/line} \cdot h_c \cdot \text{Att}/100} C_a \quad [17]$$

where  $h_c$ ,  $h_d$ , and  $h_r$  are measured in lines.

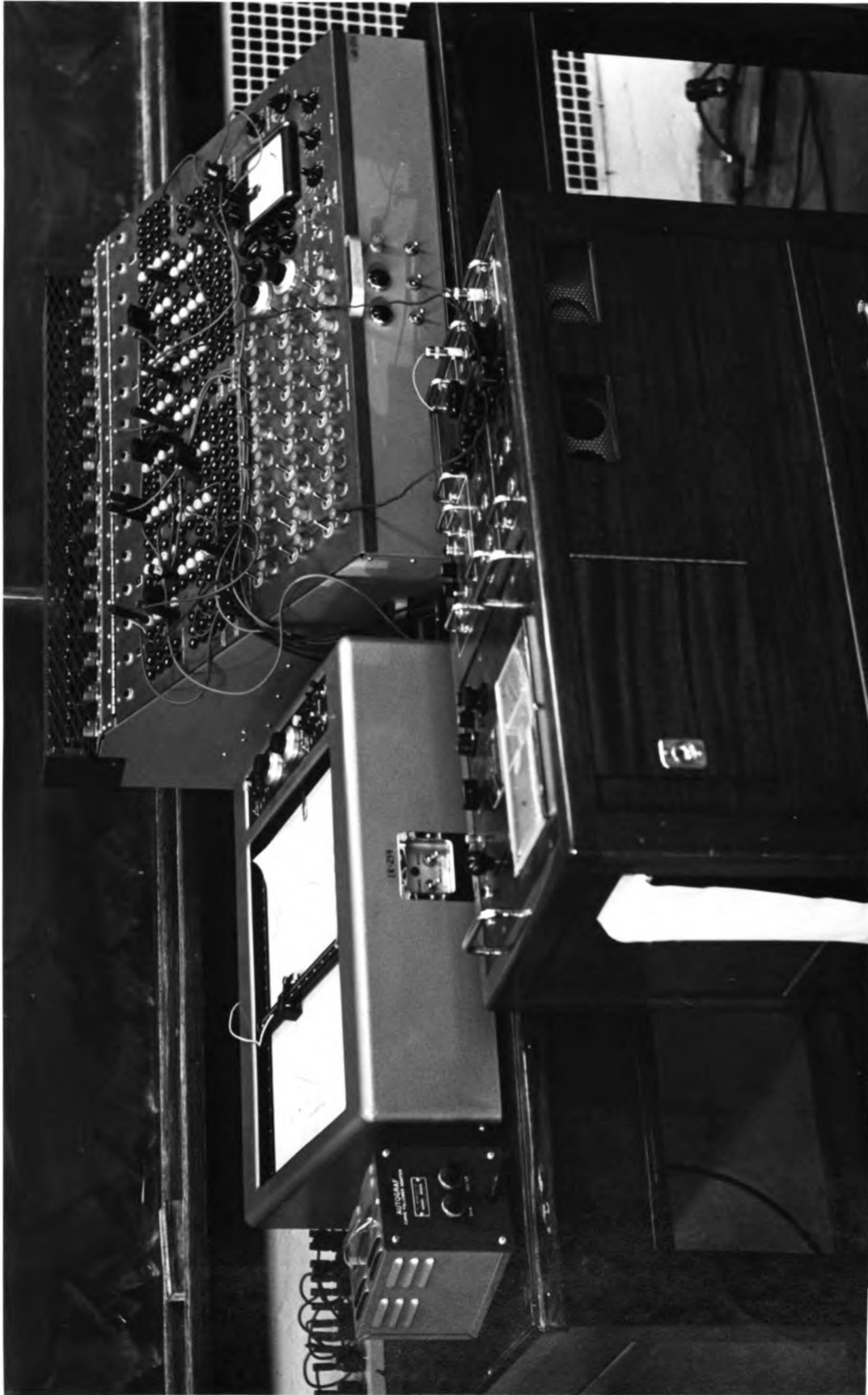


Figure 3. Equipment Used to Obtain Results

## DESCRIPTION OF EQUIPMENT

Curves

The acceleration-time curves for the ten cam contours listed in the appendix were plotted from data calculated by a digital computer. The curves were then traced with a conducting ink. The electrical resistances of these curves were between 125 ohms and 425 ohms, well below the maximum tolerable resistance of 5000 ohms.

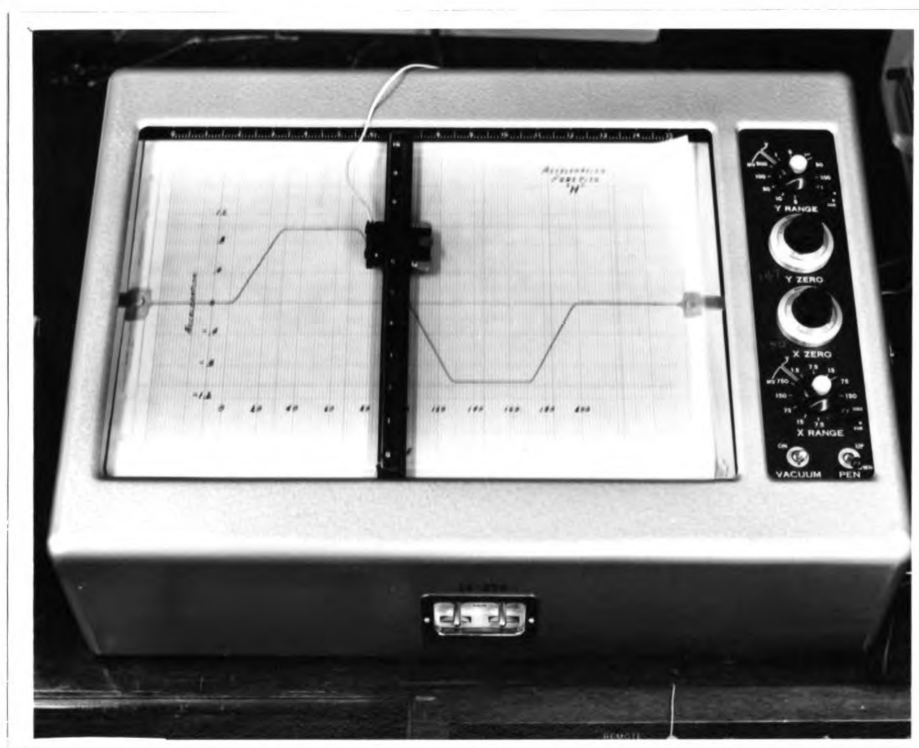


Figure 3. Function Generator and Curve

### Function Generator

An acceleration-time curve was placed on a Mosley X-Y Recorder which was converted to a function generator by means of a Curve Follower Adapter unit. The magnetic pick-up coil on the carriage was centered over the curve. The output voltage was adjusted to zero at the origin of the curve. An integrating amplifier produced a voltage which was a linear function of time. This voltage drove the carriage across the time axis at a constant rate corresponding to  $\omega_c$ , while the pick-up coil followed the curve and generated an output voltage proportional to the acceleration. This voltage was the forcing function,  $-\ddot{X}$ , of the basic differential equation [4].

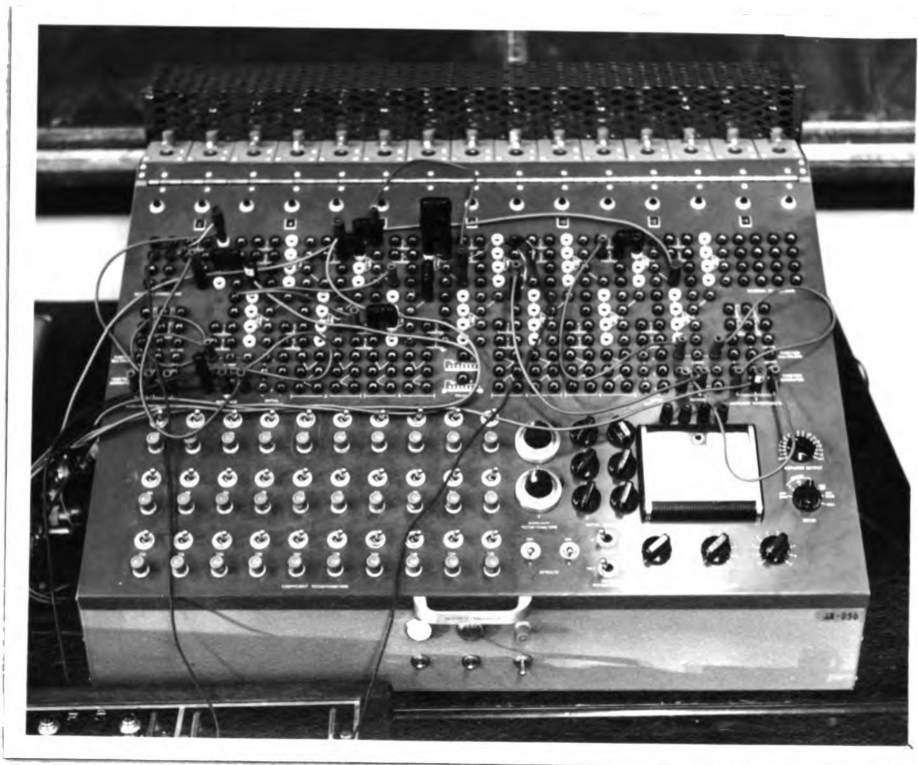


Figure 5. Differential Analyzer

### Differential Analyzer

Equation [4] was set up on the computer as shown in Figure 6. The relays D were placed across the capacitors to insure a zero charge at time zero. Another relay, E, was used to cut off the forcing function after one complete cam stroke. Potentiometer A controlled the frequency ratio,  $f$ . The solution of equation [4] was obtained from amplifier three.

### Sanborn Recorder

The results were recorded on a two channel Sanborn Oscillograph. Each channel was calibrated for a full scale deflection at a suitable voltage and attenuation factor. The voltage output of the function generator was monitored on one channel; the other channel recorded the solution of the differential equation[4].

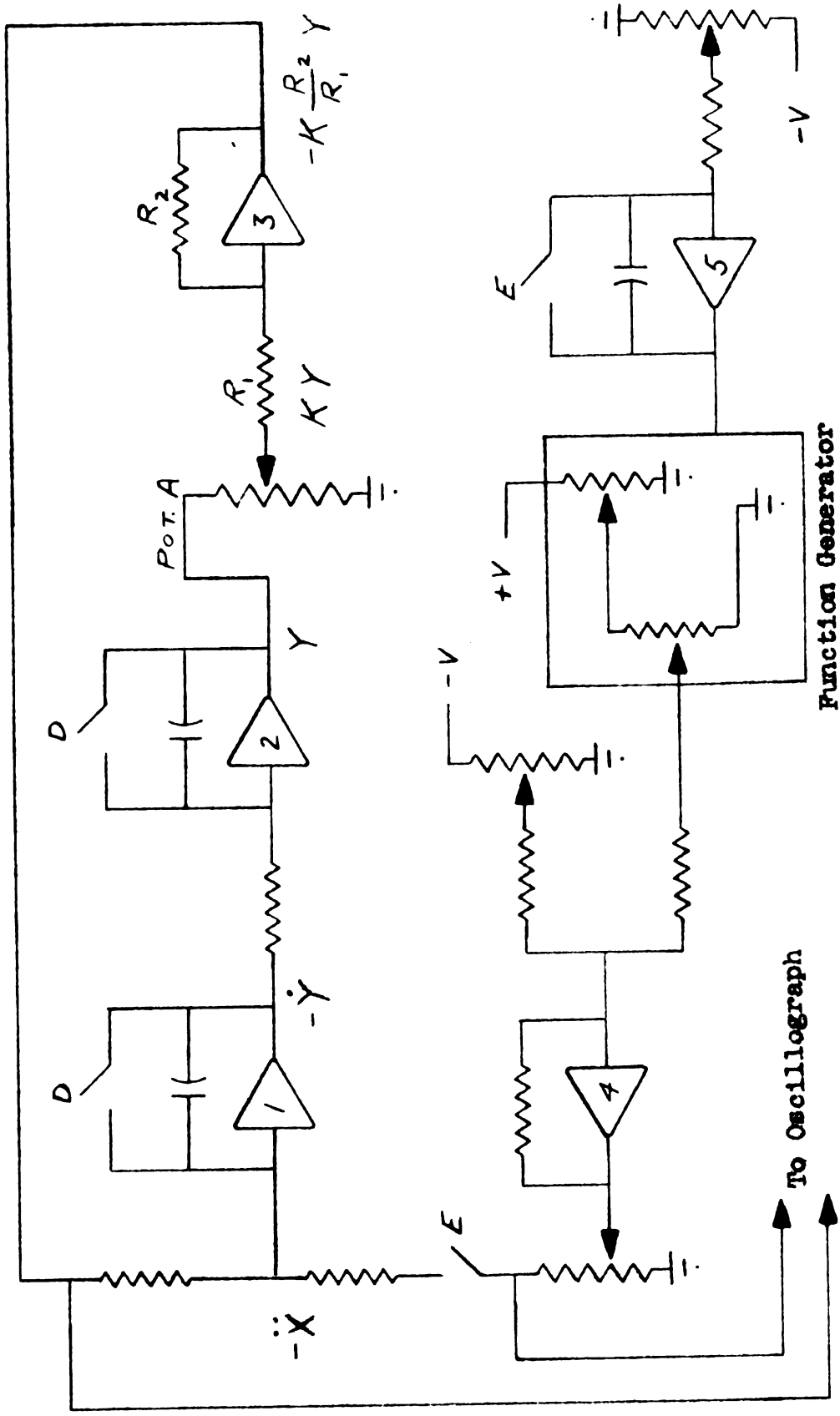


Figure 6. Schematic Diagram of Differential Analyzer Circuit

## PROCEDURE

A period of time was allowed for the equipment to stabilize. After a forty-five minute warm-up period, the following items were checked and/or adjusted: oscillograph speed and calibration,  $\omega_m$ ,  $\omega_c$ , amplifier balance, voltage supply, initial condition -  $\ddot{X} = 0$  at  $t = 0$ , and the setting K for potentiometer A.

To start the solution, relay switches D and E were turned on. Relay switch D controlled the relays across the capacitors for amplifiers one and two. Relay switch E controlled the relay across the capacitor for amplifier five and in the output line of the forcing function, -  $\ddot{X}$ . When the forcing function had completed one cycle, relay switch E was turned off thus making the differential equation [4]

$$\ddot{Y} + \omega_m^2 Y = - \ddot{X} = 0$$

which gave simple harmonic motion for the residual vibration. A sufficient number of residual vibrations were recorded to insure a good record of the residual amplitude and frequency. Relay switch D was then turned off, completing the operation. This procedure was repeated for a range of f from zero to twenty using increments of one-quarter.

## ACCURACY

Inaccuracies of the results obtained on the analog computer were expected. The errors could have been induced by one or more of the following elements. They are listed in the order of their importance:

1. the high magnification factor in amplifier three
2. stray voltage
3. rough operation of the function generator
4. amplifier drift during calculations
5. oscillograph calibration
6. measurements from recorded data
7. inherent errors in the computer

A minimum of error can be attained by constantly checking and adjusting the items listed above.

## SAMPLE CALCULATIONS

The following sample calculations were based on cam B for a frequency ratio,  $f$ , of 6.5 and  $C_a = 5.333$ .

To obtain the frequency ratio,  $f$ , the following setting  $K$  was made on potentiometer A. From equation [7]

$$f = \frac{\omega_m}{\omega_c} \quad [7]$$

$\omega_c$  was selected to be unity, therefore

$$f = \omega_m \quad [18]$$

The following resistors were chosen:

$$\begin{aligned} R_2 &= 10 \text{ megaohms} \\ R_1 &= 0.1 \text{ megaohms} \end{aligned}$$

Referring to Figure 6

$$\omega_m^2 = K \frac{R_2}{R_1} = K 100 \quad [19]$$

For the nominal value,  $f = 6.5$  and from equations [7] and [19]

$$f^2 = 6.5^2 = 42.3 = K 100$$

therefore

$$K = 0.423$$

The following data were obtained from Figure 2.

$$L_c = 6.2 \quad \text{in.}$$

$$L_m = 0.87 \quad \text{in.}$$

$$h_c = 10 \quad \text{lines at attenuation 100}$$

$$h_d = 22.9 \quad \text{lines at attenuation 100}$$

$$h_r = 15.2 \quad \text{lines at attenuation 100}$$

From equation [13]

$$f = \frac{6.2}{.87} = 7.12$$

From equation [16]

$$S_d = \frac{1 \times 22.9}{1.1 \times 10} \cdot 5.333 = 11.1$$

and from equation [17]

$$S_r = \frac{1 \times 15.2}{1.1 \times 10} \cdot 5.333 = 7.36$$

Values obtained in this manner were used to plot the curves displayed in the Discussion of the Results.

## DISCUSSION OF RESULTS

### Comparison With Published Results

The residual stress factor curves given by other investigators were plotted in this report for all ten cams. These curves were used to check the results obtained on the analog. When the results compared favorably, this was a good indication that the dynamic stress factor curves were accurate. The results obtained for  $S_r$  compared very well except for cam G. It was assumed that a large stray voltage induced the error.

In some instances there was a large percentage of error when values of  $S_r$  calculated in this study were compared with those given by other investigators. These large percentage errors in  $S_r$  occurred only for large values of  $f$  where  $S_d$  was much larger than  $S_r$ . A large percentage error in  $S_r$  did not necessarily imply a large percentage error in  $S_d$ . This followed because the small absolute error which corresponded to a large percentage error in  $S_r$  was but a small percentage error of  $S_d$ . For values of  $f$  less than seven or thereabouts, good accuracy was obtained.

### Residual Stress Factor

Although no new information was obtained concerning the residual stress factors, this section of the report was

important as is it verified the results of other investigators. These curves are displayed in Figures 7--16.

For purposes of discussion, the cams were divided into five groups. The uncompensated seventh degree polynomial cam is discussed first because it will be used as the basis of comparison for the other cams. This cam stood out from all the others because of its extremely low residual stress factor. In this respect, it was even superior to the cycloidal cam for all values of  $f$  greater than three.

The second group consisted of cams A and B. These cams had acceleration specifications in trigonometric form. These cams displayed generally higher residual stress factors than the polynomial. However, cam A showed very good characteristics for values of  $f$  greater than eleven. Cam B showed good results in the range of  $f$  between ten and fifteen.

The third group consisted of cams C and E, having exponential acceleration specifications. Cam C showed generally inferior results for all values of  $f$  while cam E displayed good results for all values of  $f$  greater than fourteen.

A fourth group having quadratic acceleration specifications, consisted of cams F, G, and H. Cams F and H showed generally poor results while cam G displayed very good results for all values of  $f$  greater than twelve with the exception of a small region of  $f$  near fifteen.

The fifth group consisted of the double and triple cycloid cams. Although the double cycloid generally had a lower residual stress than the triple cycloid, both cams were inferior to the polynomial.

#### Dynamic Stress Factor

It was very interesting to note the similarity between a residual stress curve and its corresponding dynamic stress curve. When peaks occurred in the residual stress curve, peaks were present in the dynamic stress curve. Similarly, when low values of  $S_r$  persisted for ranges of  $f$ , low values of  $S_d$  were also present for the same range. For large values of  $f$ , the system approached the characteristics of a rigid body and for all practical purposes the dynamic stress was larger than the residual stress by a factor equal to  $C_a$ .

The polynomial curve displayed good dynamic stress characteristics for all practical values of  $f$ . It was generally superior to all the cams studied in this thesis for  $f$  ranging from two to eight. This range is especially important for high speed operation. However, due to its large acceleration coefficient, several other cams displayed better dynamic characteristics in the higher ranges of  $f$ . The double cycloid showed excellent results for the frequency range greater than five. The triple cycloid showed very good results compared to the polynomial for  $f$  greater than eight. Cams A and B also displayed excellent results for  $f$

greater than ten. The remaining cams, C, E, F, G, and H displayed generally inferior characteristics.

### Relationship Between Curves

The difference between the residual stress and dynamic stress was observed to be a function of the maximum acceleration coefficient and the frequency ratio. To relate the two curves an empirical equation was sought. The equation was required to satisfy the following conditions:

1. The results of the empirical equation were to be conservative.
2. The following boundary conditions were to be satisfied.
  - A.  $S_d > S_r$  for  $f > 1$
  - B.  $S_d$  approached  $S_r + C_a$  as  $f$  approached infinity

Several empirical equations were tried and the most satisfactory equation developed was

$$S_d = S_r + C_a \left[ 1 - \frac{1}{f} \right] \quad [20]$$

To satisfy the above conditions certain restrictions were placed on equation [20]. For calculating  $S_d$  from equation [20] no values of  $f$  less than one were used. In addition, for the range of  $f$  between one and eight only certain points were used. The points that were omitted were those giving the curve a positive slope. This is clarified in Figure 17, where results using equation [20] were compared with those calculated on the analog.

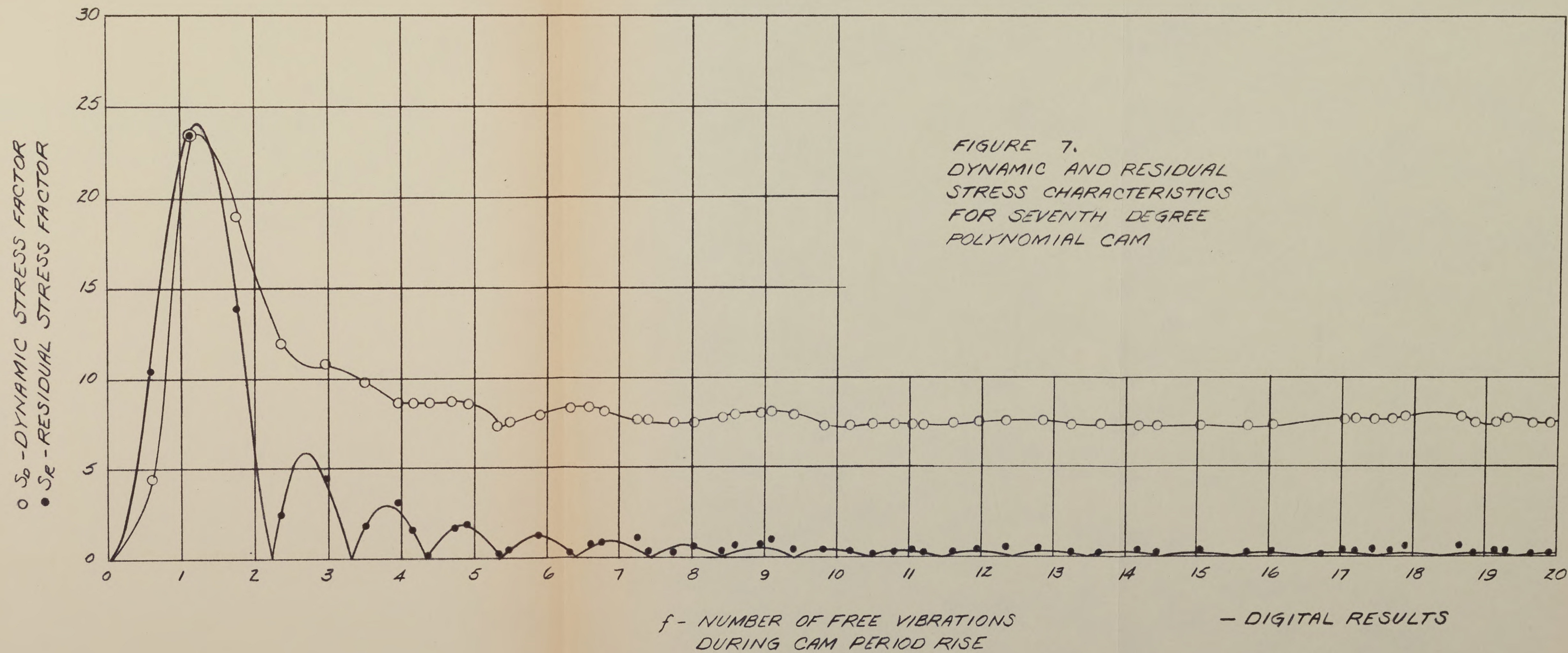
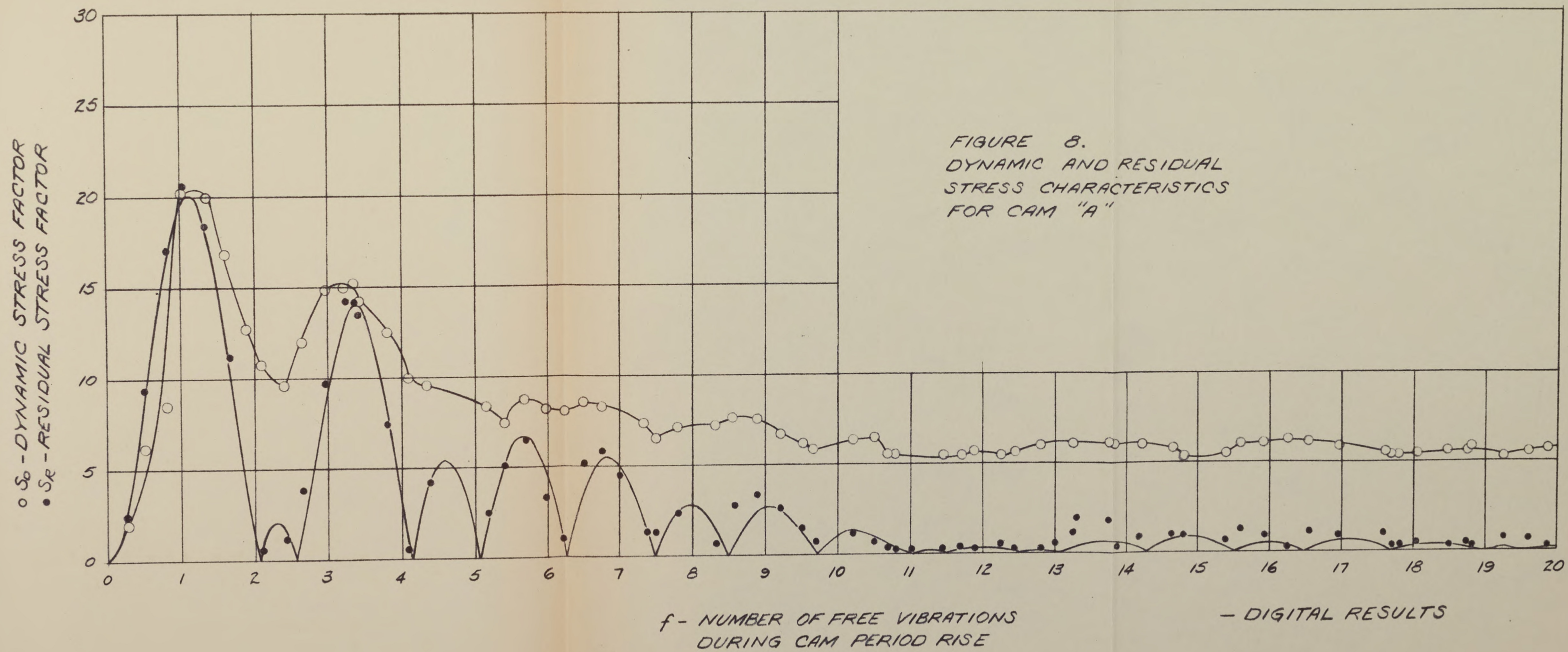
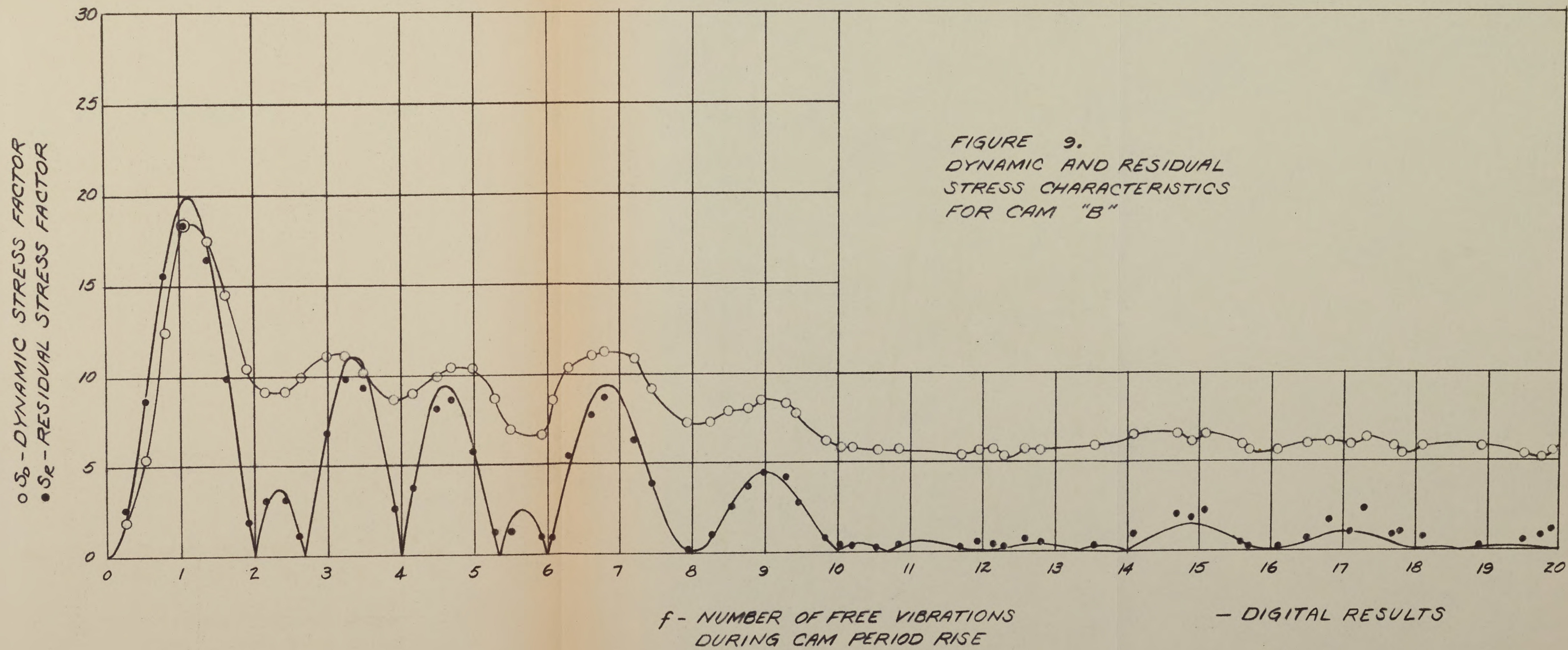
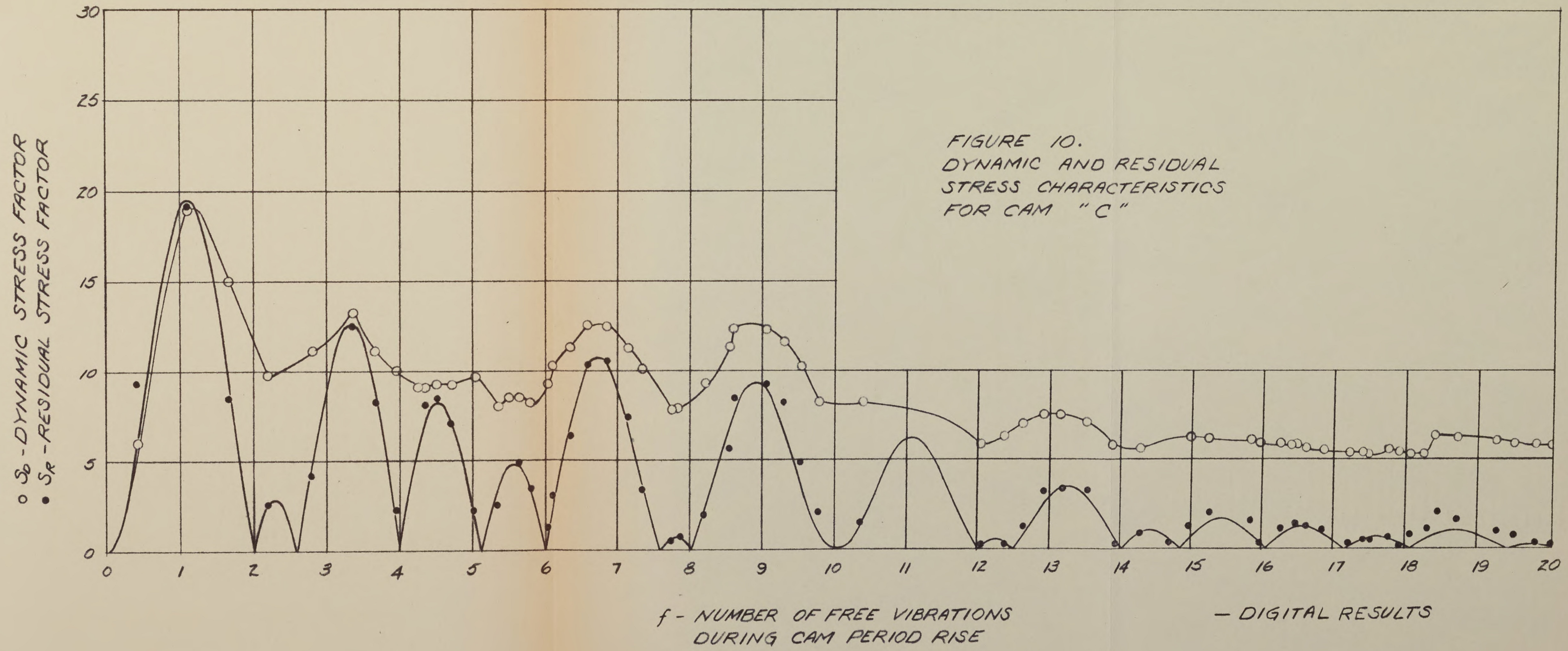
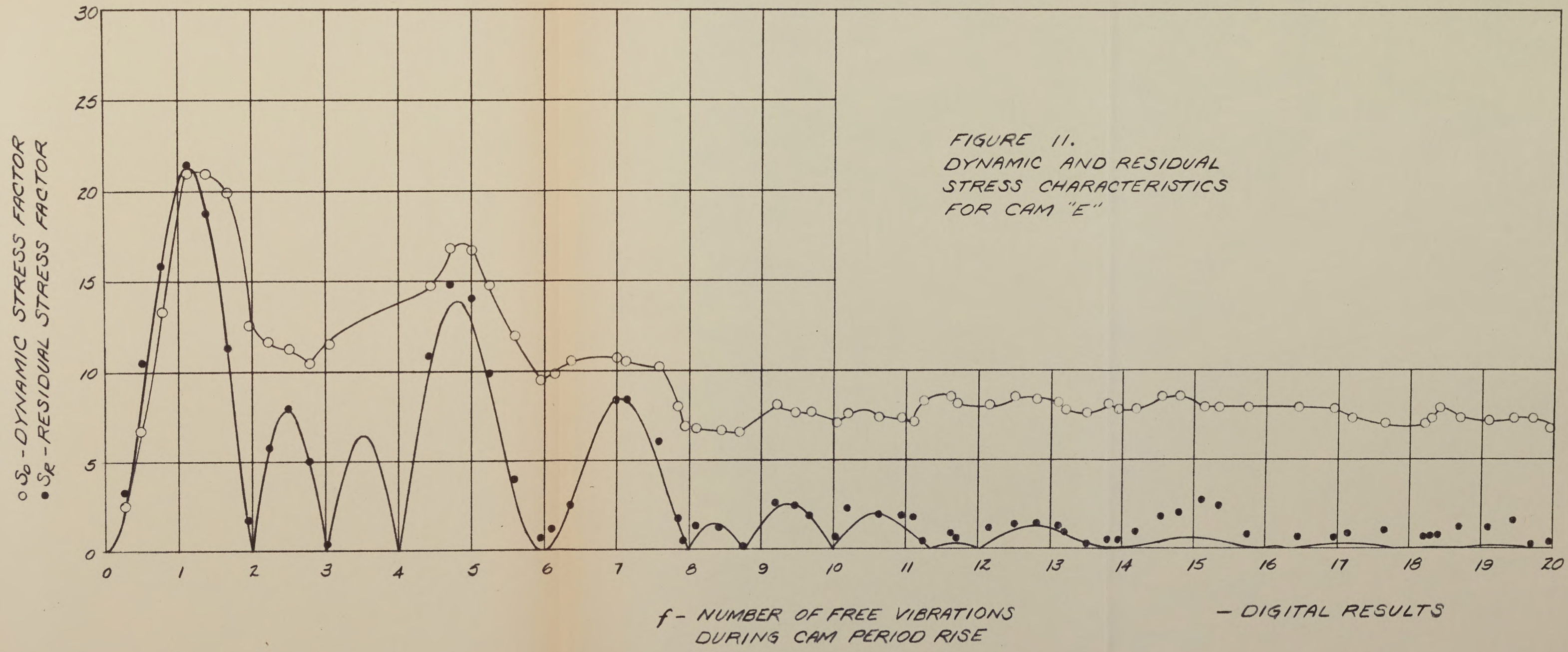


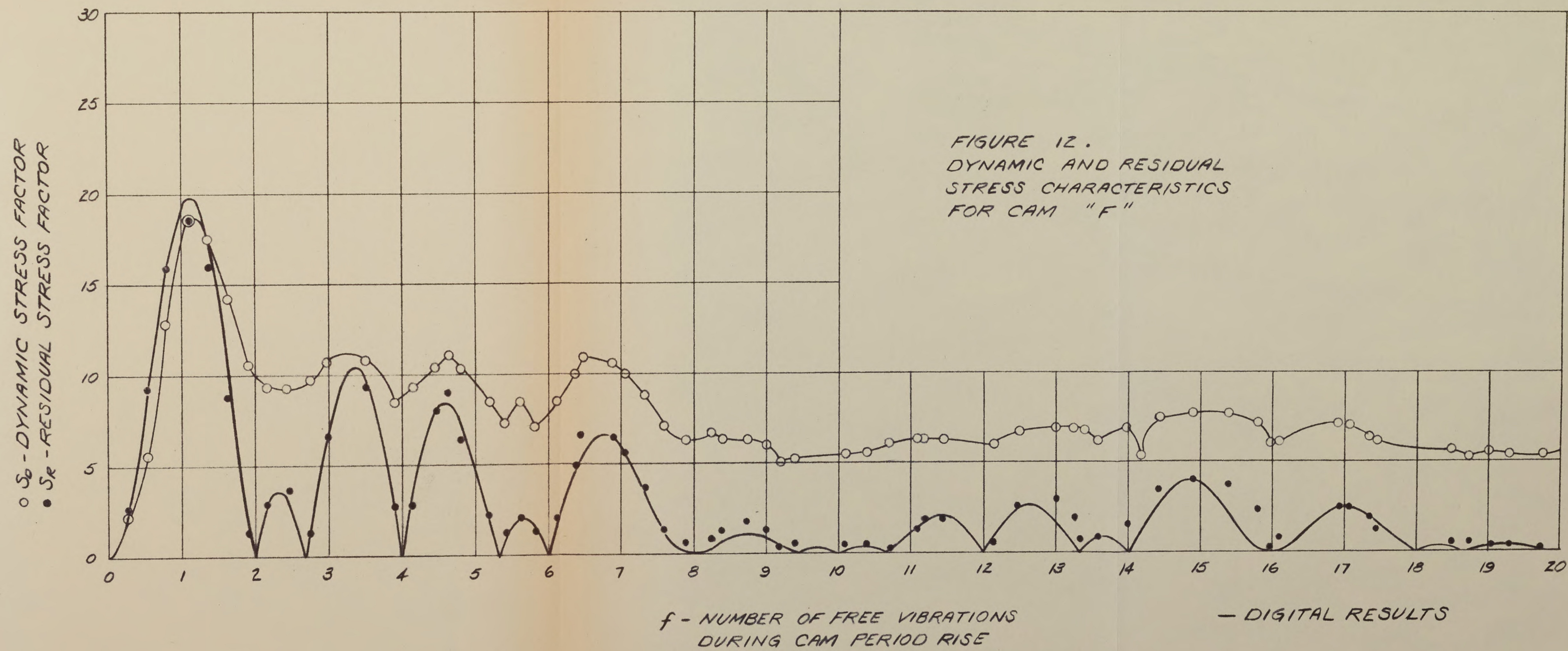
FIGURE 7.  
 DYNAMIC AND RESIDUAL  
 STRESS CHARACTERISTICS  
 FOR SEVENTH DEGREE  
 POLYNOMIAL CAM

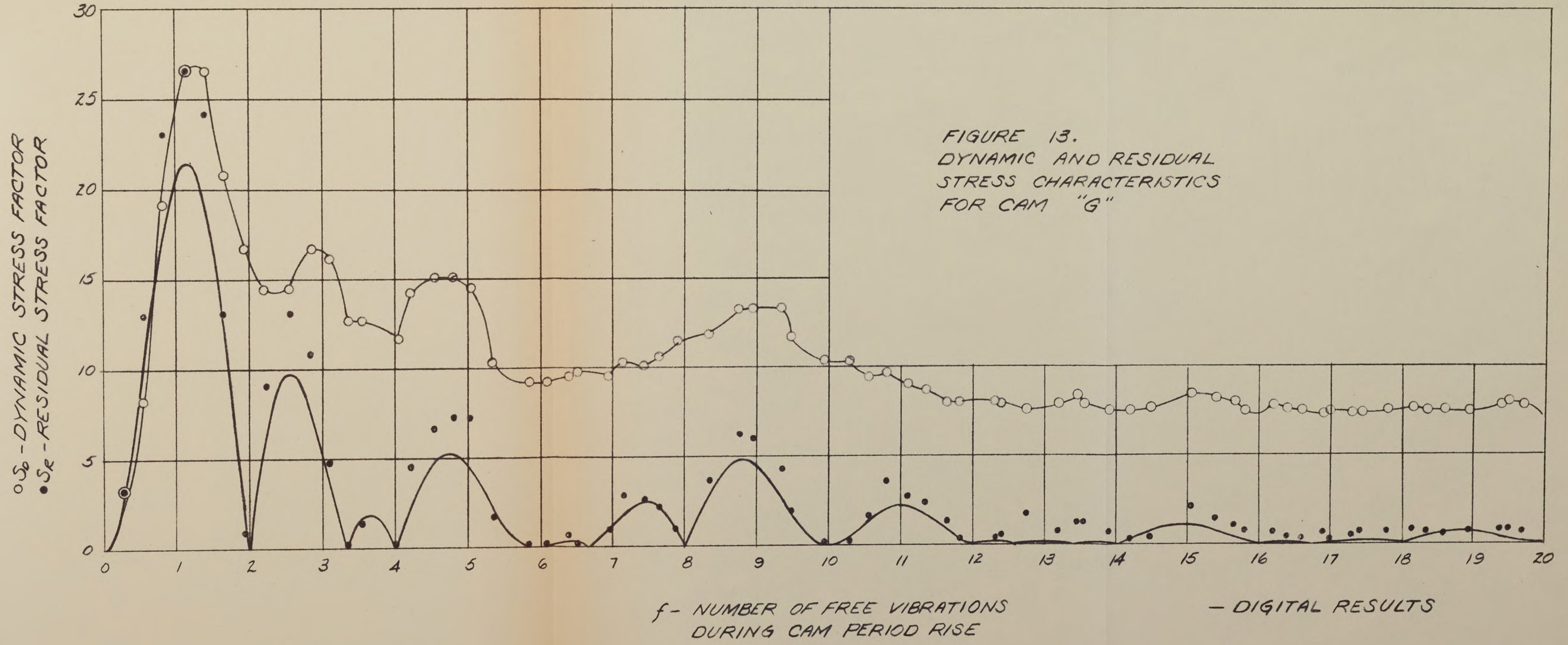


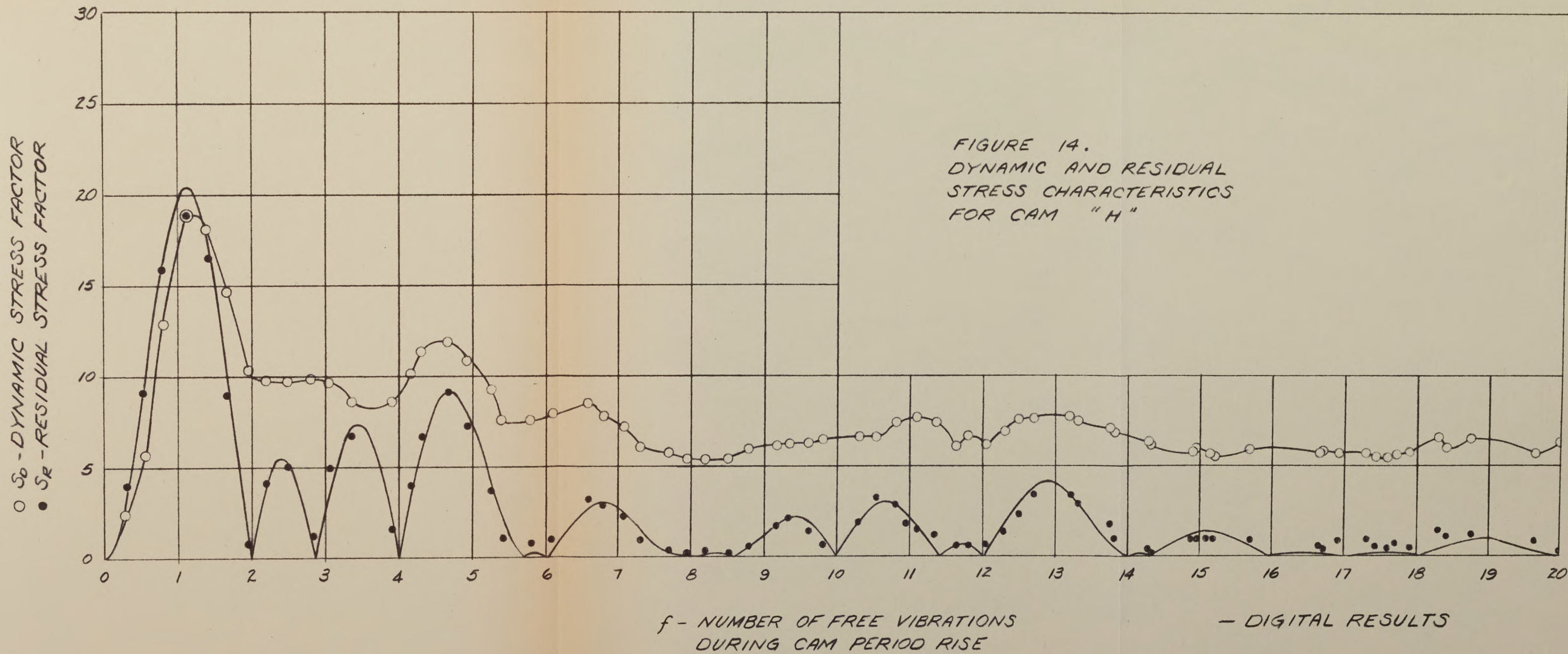


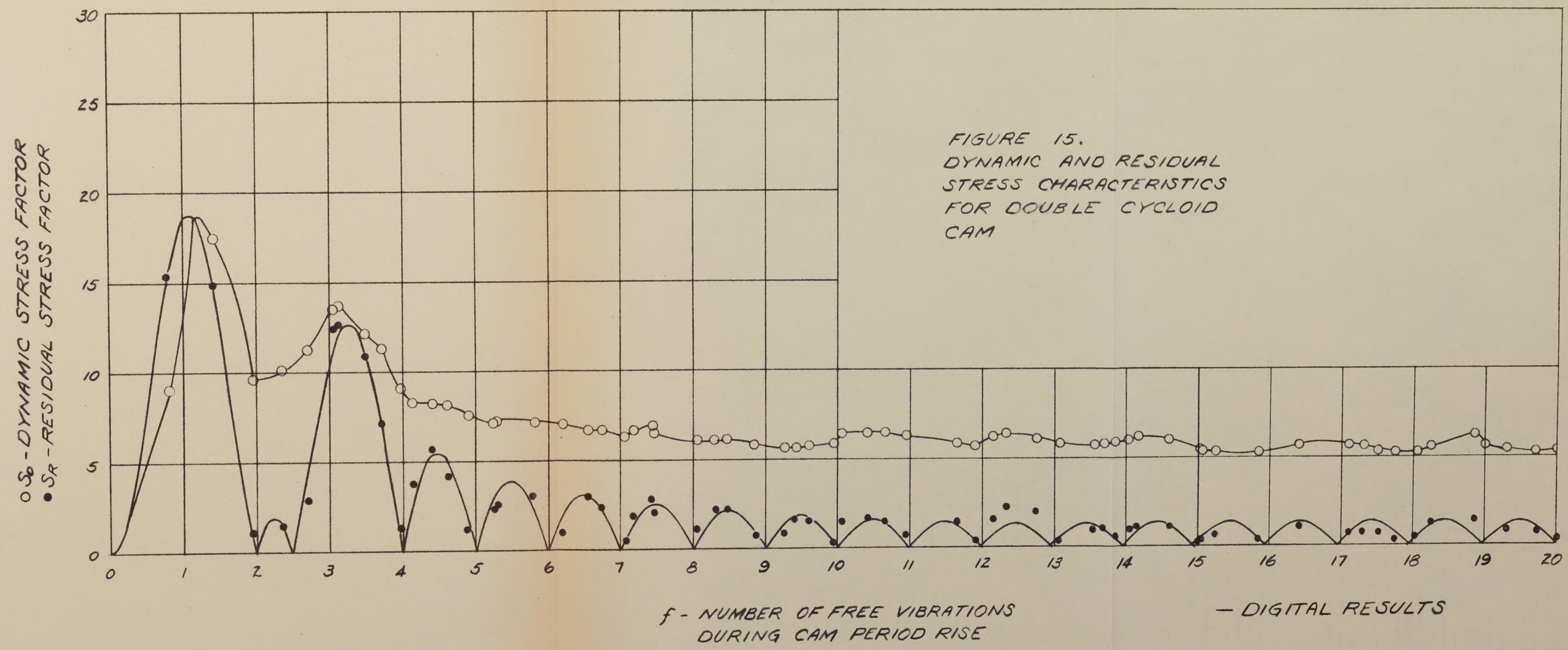


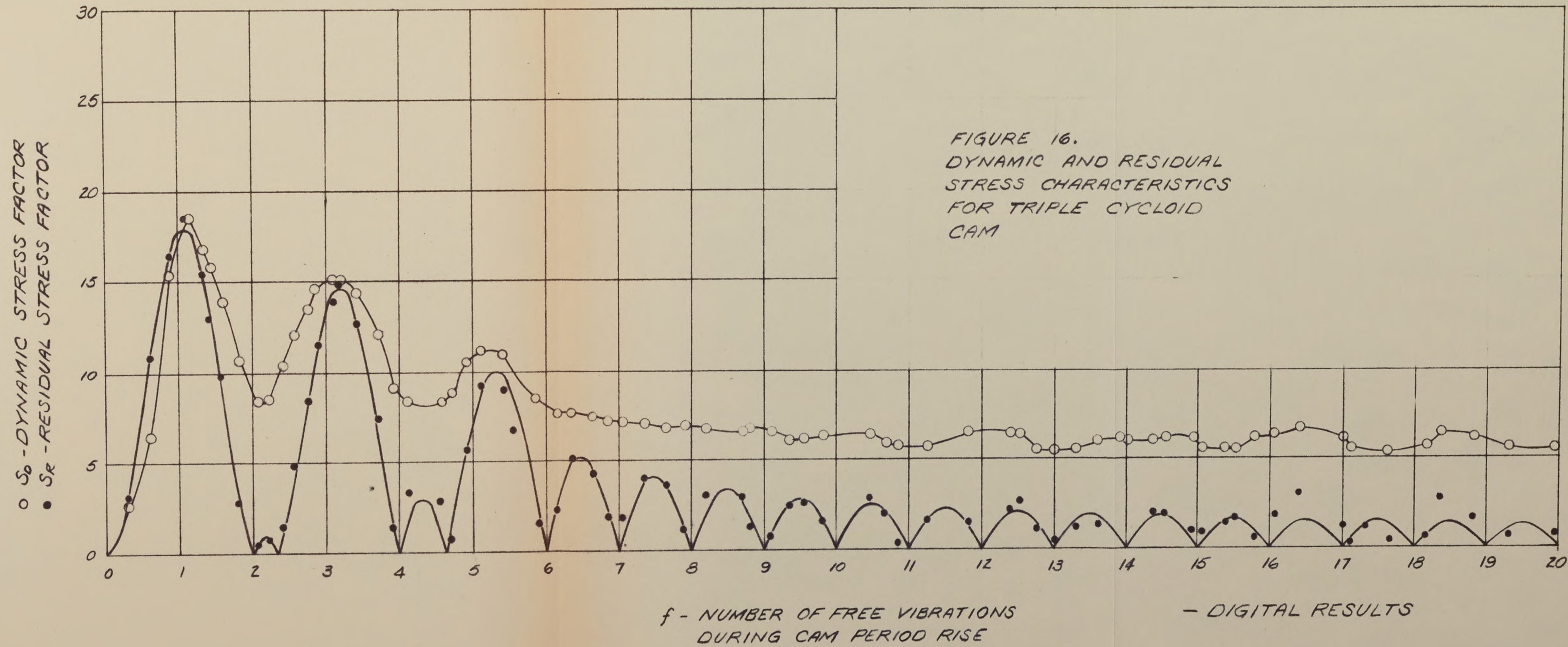


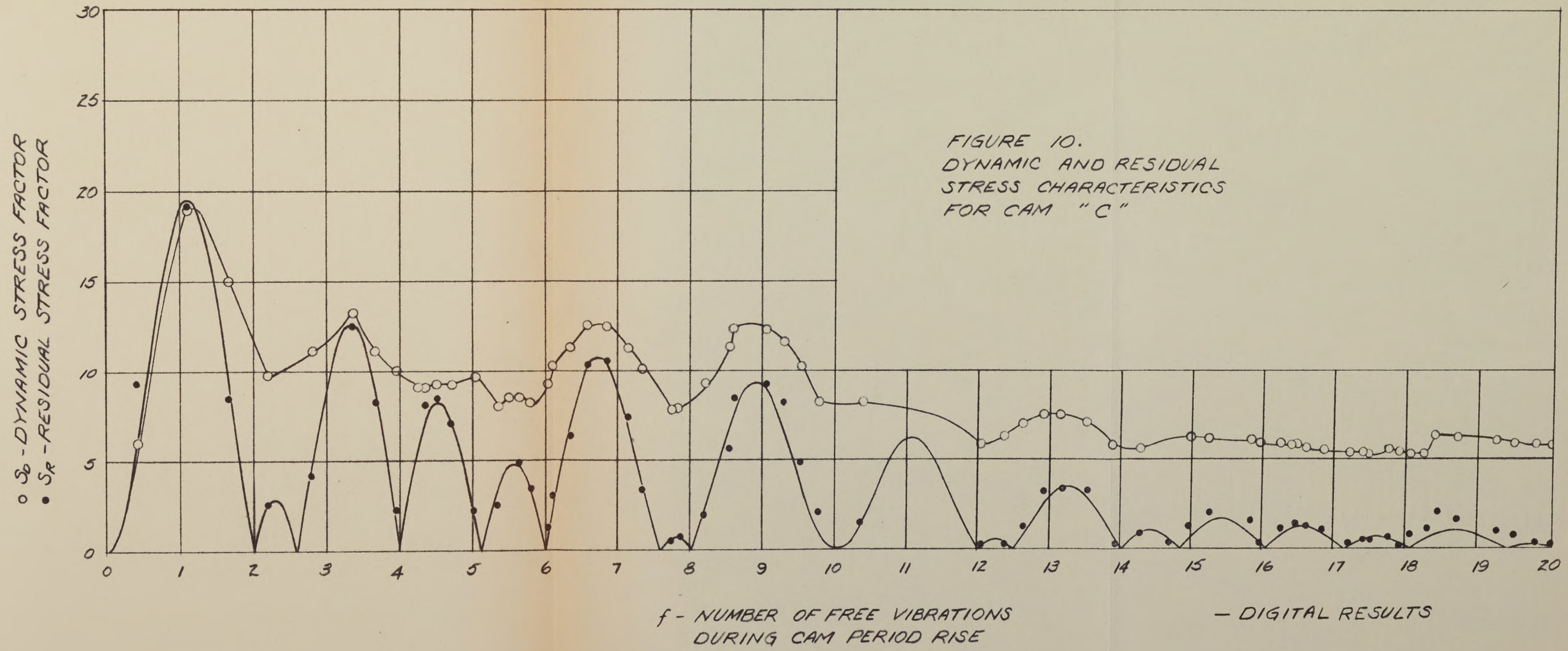


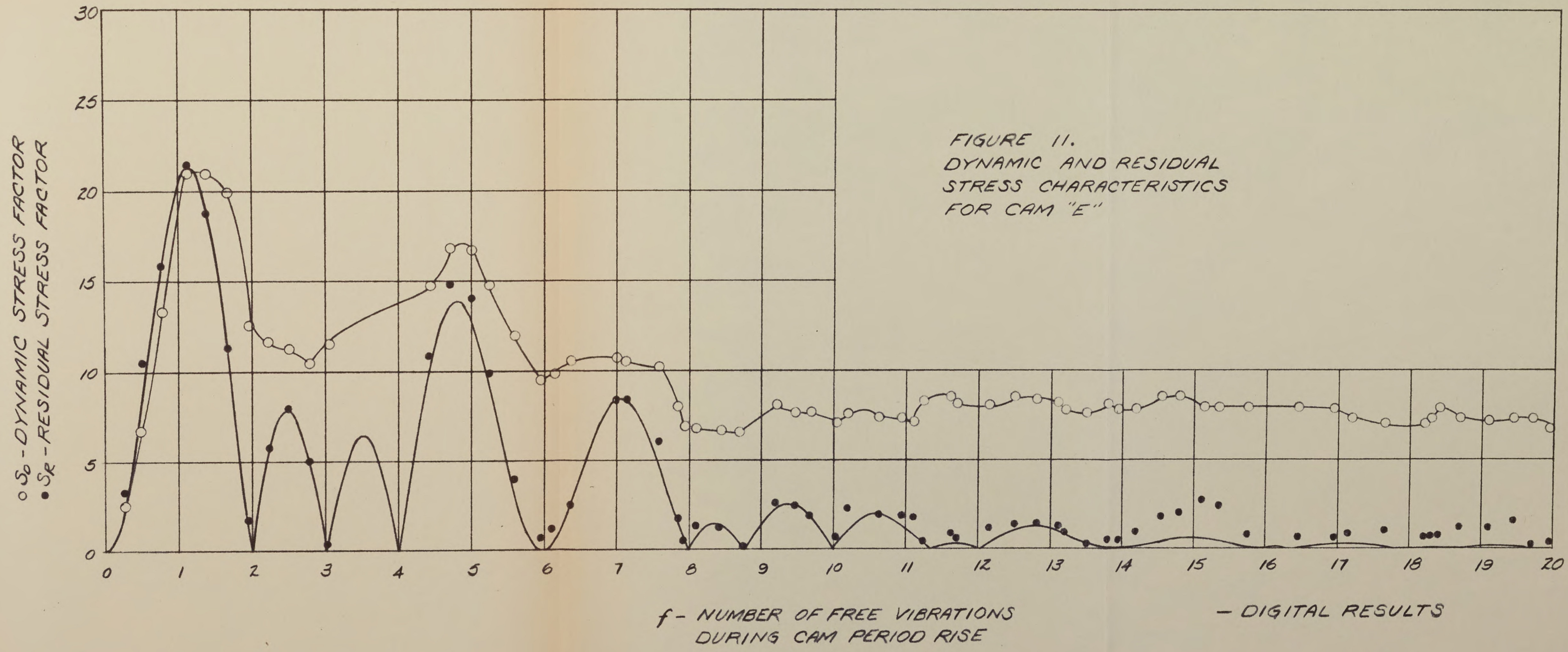


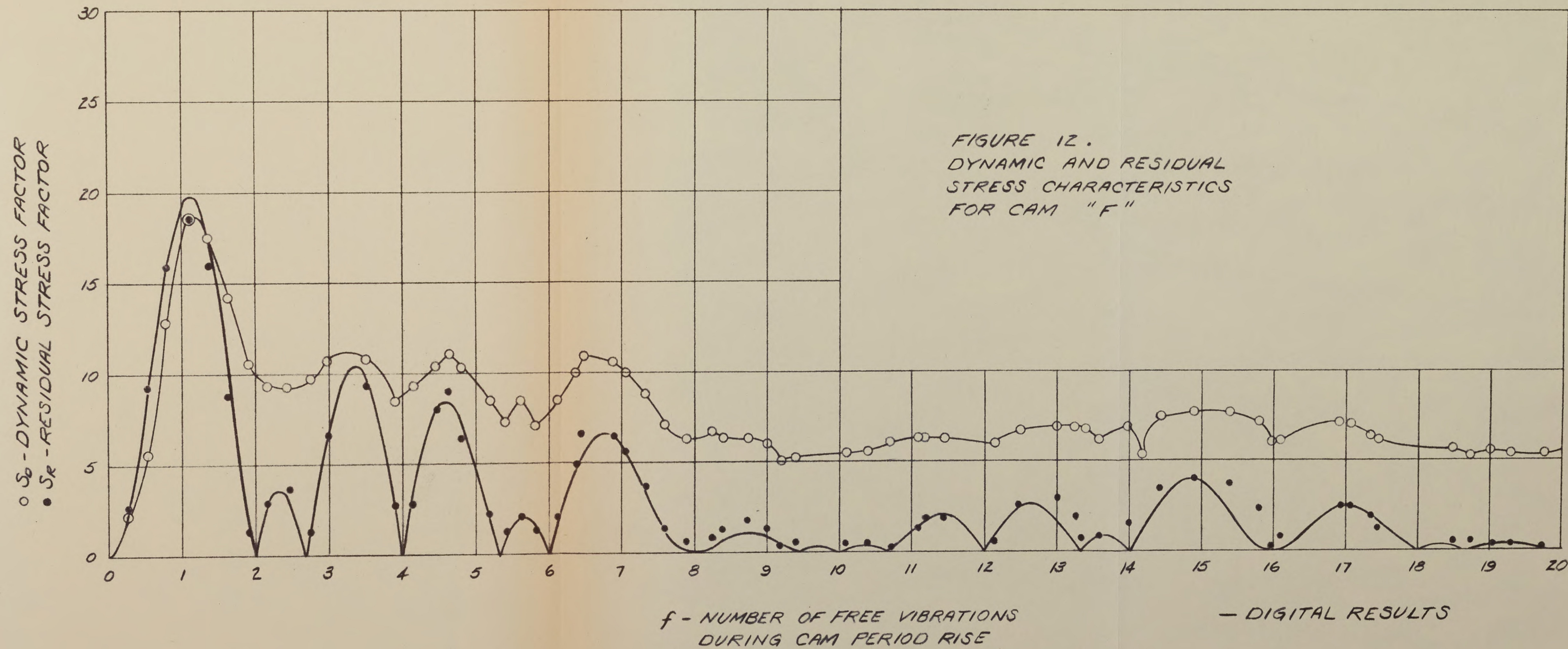


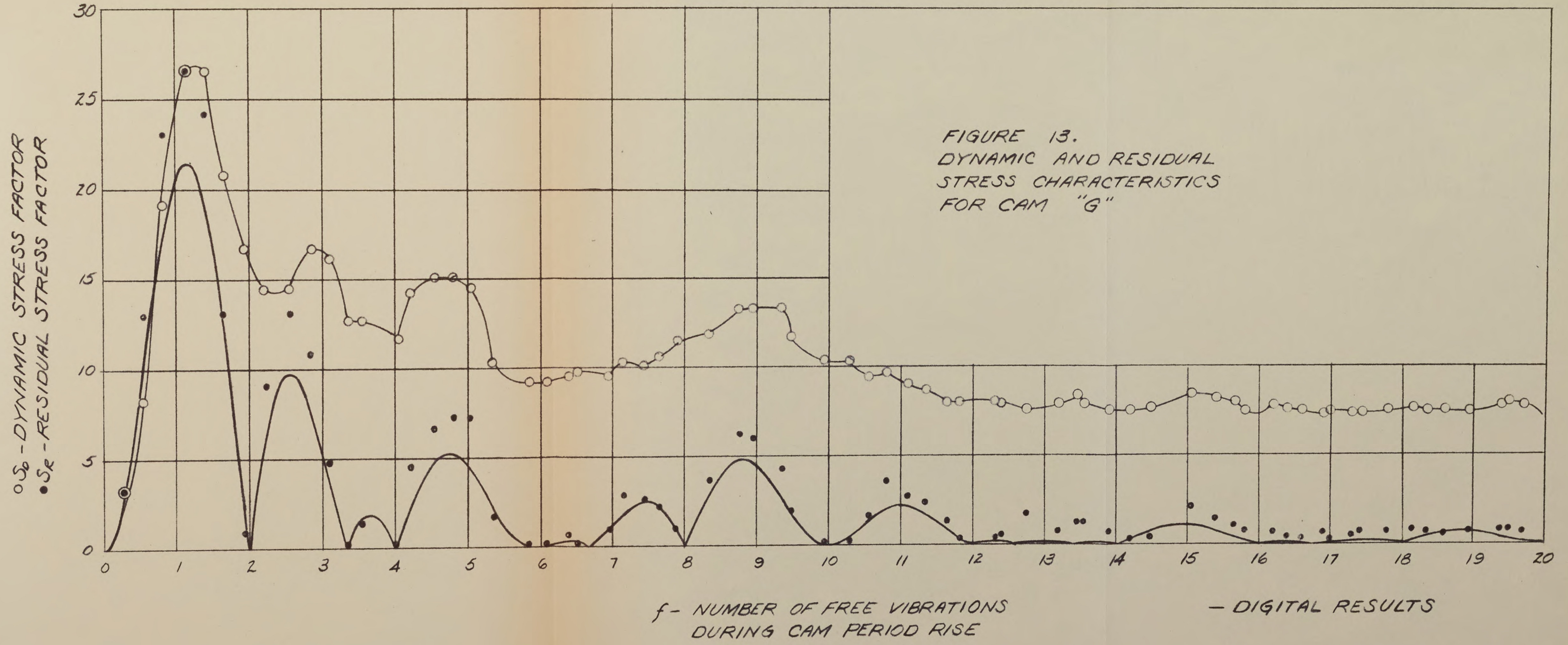


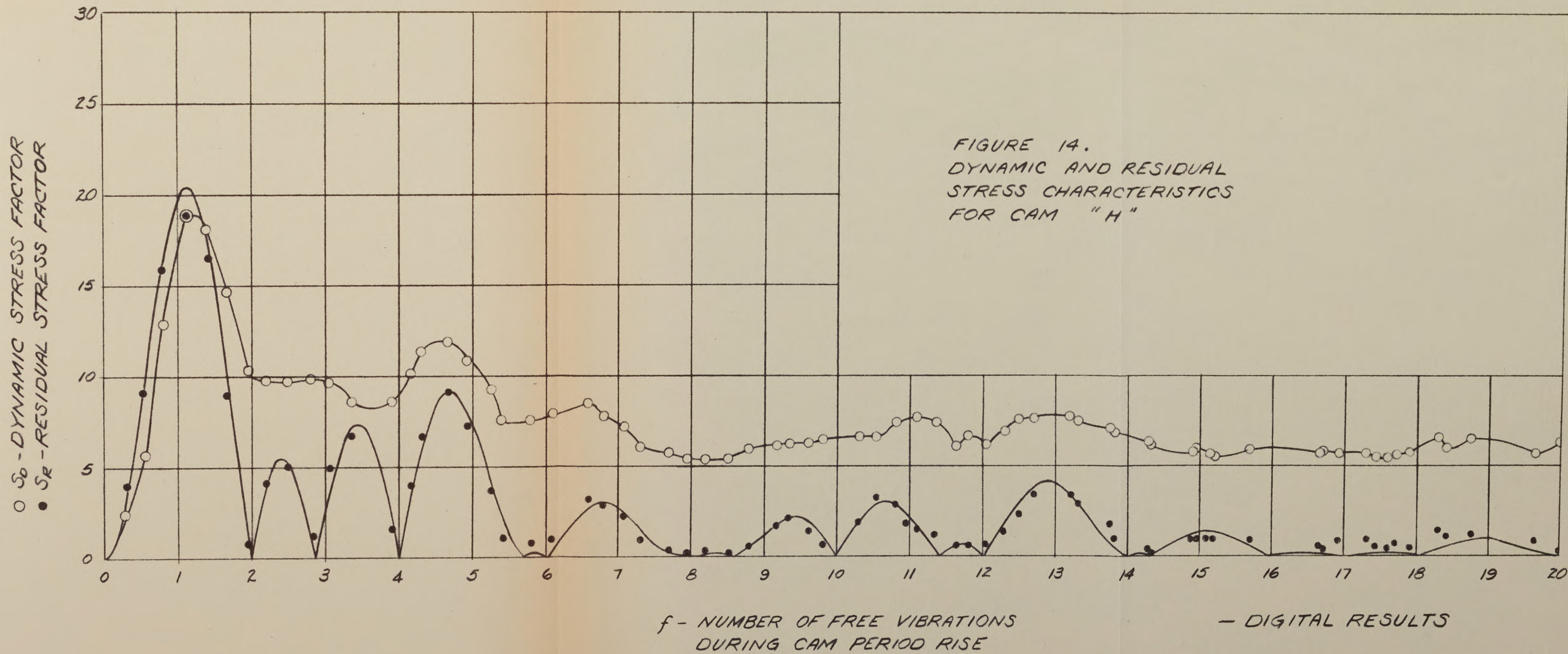












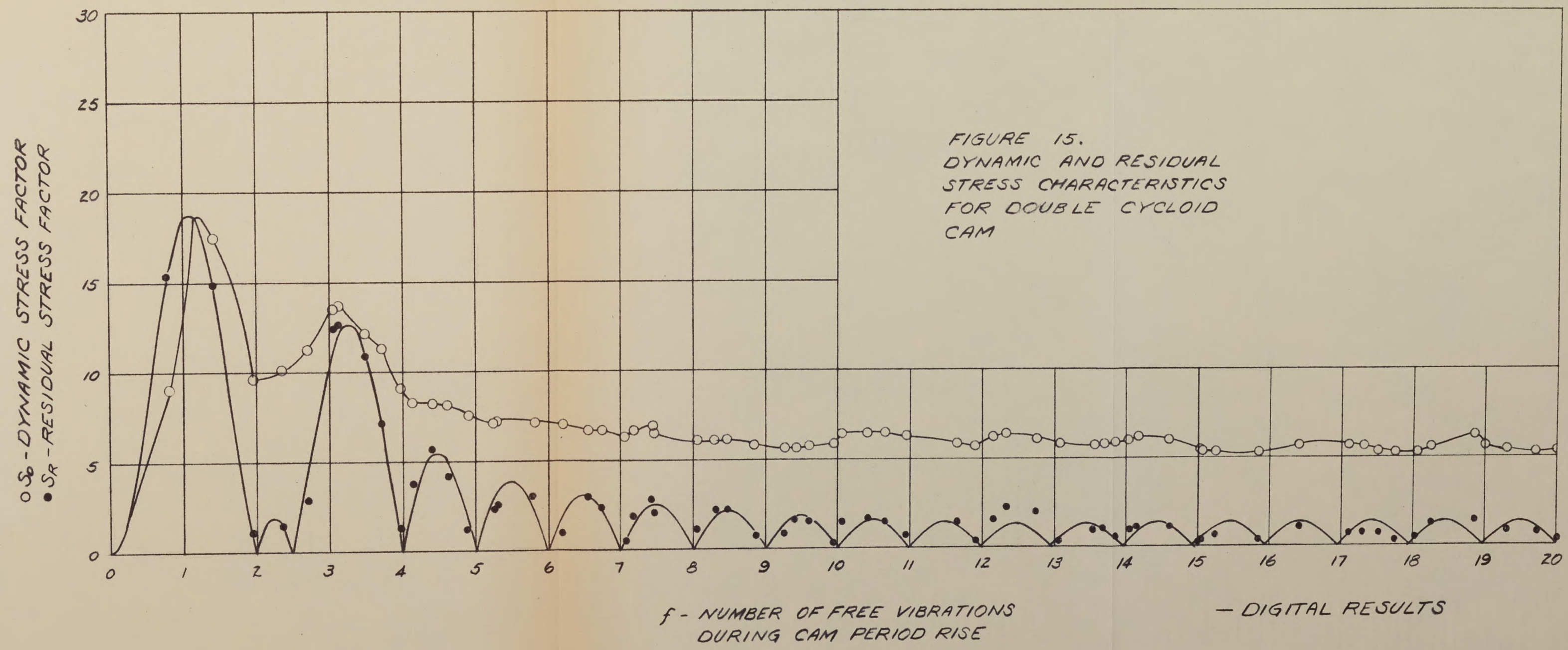
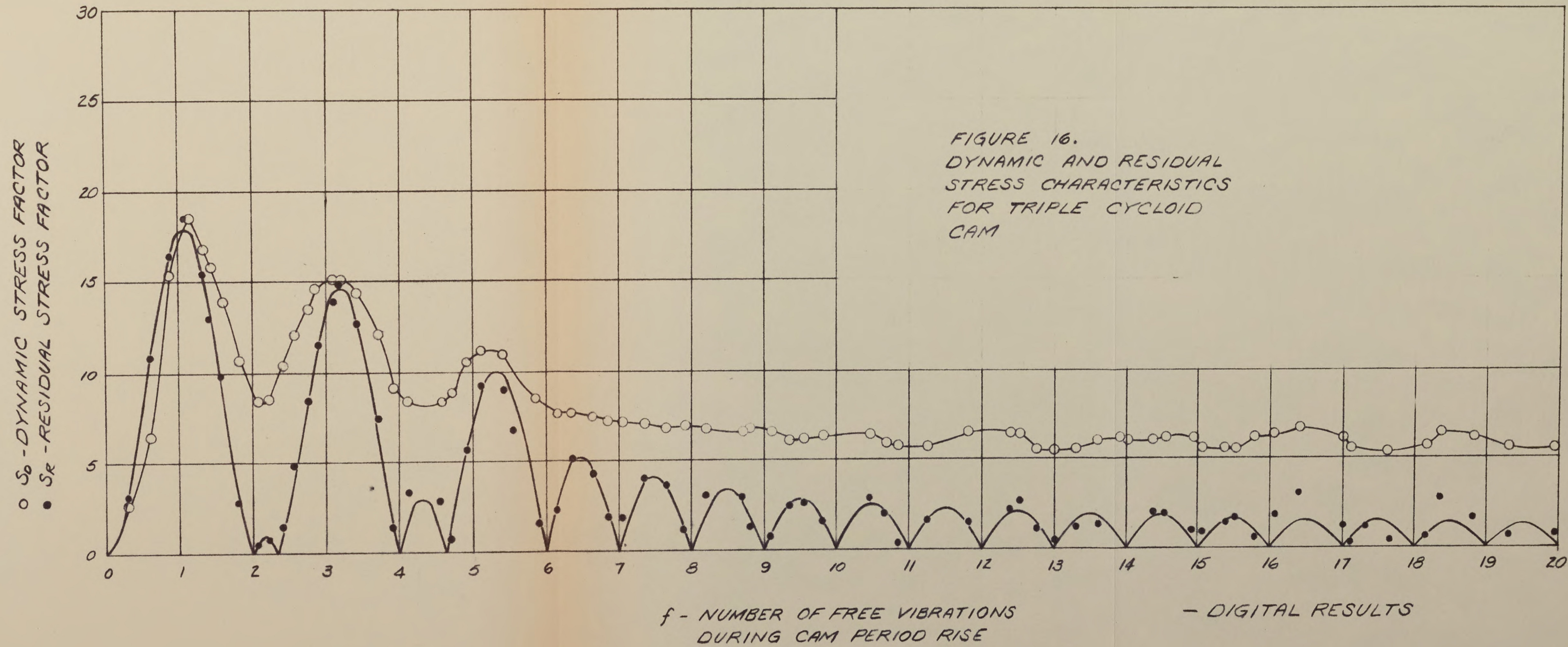
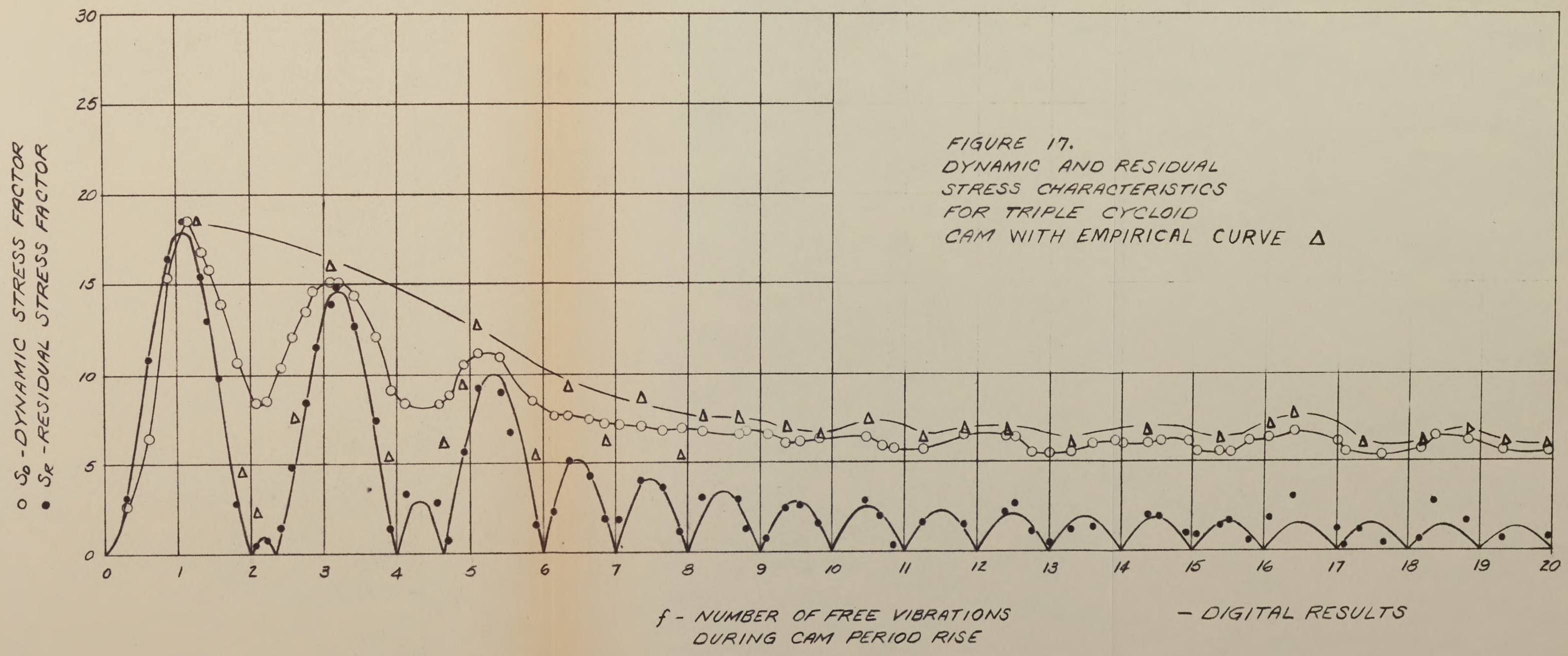


FIGURE 15.  
DYNAMIC AND RESIDUAL  
STRESS CHARACTERISTICS  
FOR DOUBLE CYCLOID  
CAM





## CONCLUSIONS

The research reported in this thesis resulted in three significant contributions. First, the results verified residual stress factors reported by other investigators. Second, dynamic stress factors were found for ten cam contours. And finally, a correlation between the dynamic and the residual stress factors was found. This correlation was in the form of the empirical equation

$$S_d = S_r + C_a \left[ 1 - \frac{1}{f} \right] \quad [20]$$

Having found and expressed a correlation between  $S_r$  and  $S_d$ , it is now possible for designers to calculate the maximum dynamic stress during a cam stroke simply and quickly. Through the use of equation [20] maximum stresses can be predicted without making a detailed and time consuming analysis.

Results also showed that for mechanisms brought to a positive stop after the cam stroke, a preference for one cam over another should not be based on the residual stress factor alone. As previously mentioned, the residual stress factors for the polynomial cam were far superior to other cams. However, for certain ranges of  $f$  several other cams had lower dynamic stresses. This was due to a difference



in the maximum acceleration coefficient. Therefore, a compromise should be made between  $C_a$  and  $S_r$  when selecting a cam for such applications.

## POSSIBILITIES FOR FUTURE STUDIES

Equation [20] was based on the results of ten cam contours having diverse acceleration specifications. Therefore, it is probable that this equation is adequate for all cam contours. A possibility for future investigations is to determine the maximum stress for other cams for the purpose of checking the adequacy of equation [20]. Another possibility is to find a more exact relationship between  $S_d$  and  $S_r$  through the use of digital computing facilities.

## BIBLIOGRAPHY

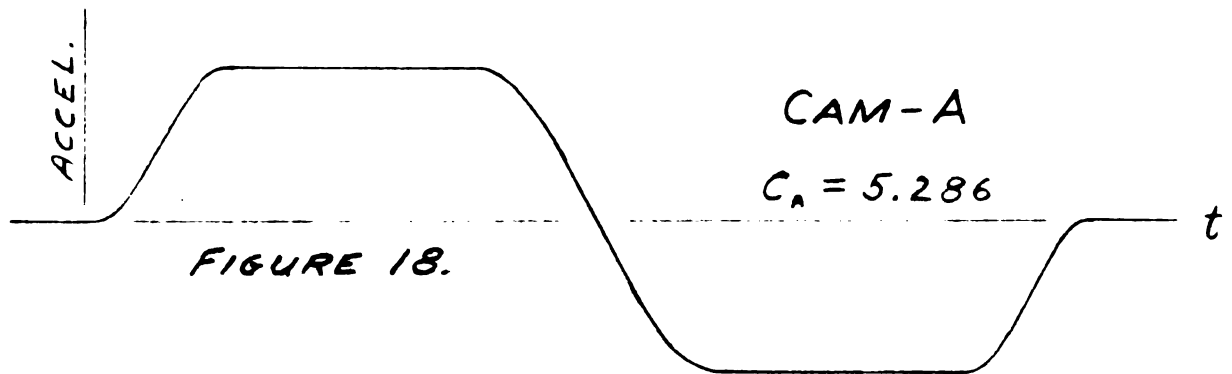
1. Anderson, D. G. "Cam Dynamics," Product Engineering, 24 (Oct., 1953), pp. 170-176.
2. Dudley, W. M. "A New Approach to Cam Design," Machine Design, 19 (July, 1947), pp. 143-48, 184.
3. Hrones, John A. "Cam Design and Application," Part III, Machine Design, May, 1949, pp. 107-112, 178.
4. Kloomok, M. and R. V. Muffley. "Plate Cam Design With Emphasis on Dynamic Effects," Product Engineering, 26, Part I (Feb.), pp. 156-62.
5. Mercer, Jr., S. and A. R. Holowenko. "Cam Forms Calculated by the Digital Computer," ASME Paper 57-A-42, December, 1957.
6. Mercer, Jr., S. "Cam Dynamics," Michigan State University Engineering Experimental Station, 1958.
7. Mitchell, D. B. "Cam Follower Dynamics," Machine Design, May, 1949, pp. 151-54.
8. Neklutin, C. N. "Vibration Analysis of Cams," Transactions of the Second Conference on Mechanisms. Reprinted from Machine Design, December, 1954.
9. Rothbart, Harold A. "Cam Dynamics of High Speed Systems," Machine Design, March, 1956, pp. 100-107.



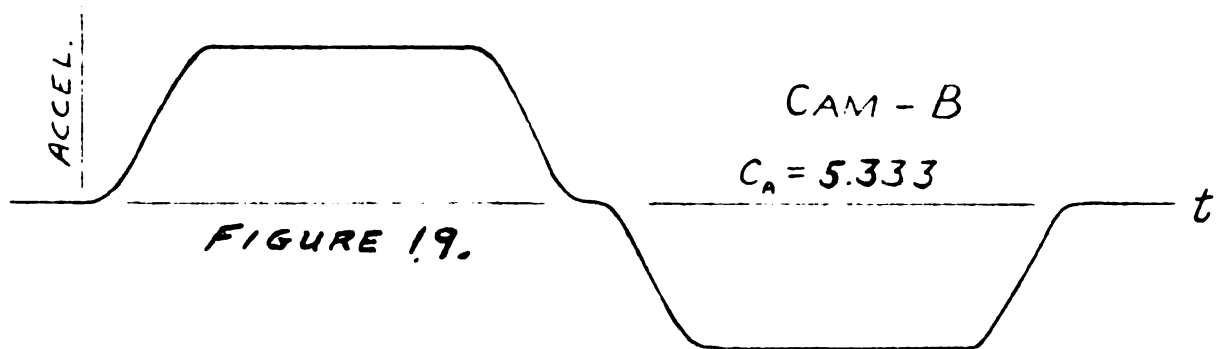
APPENDIX

ACCELERATION SPECIFICATIONS OF  
THEORETICAL CAM CONTOURS

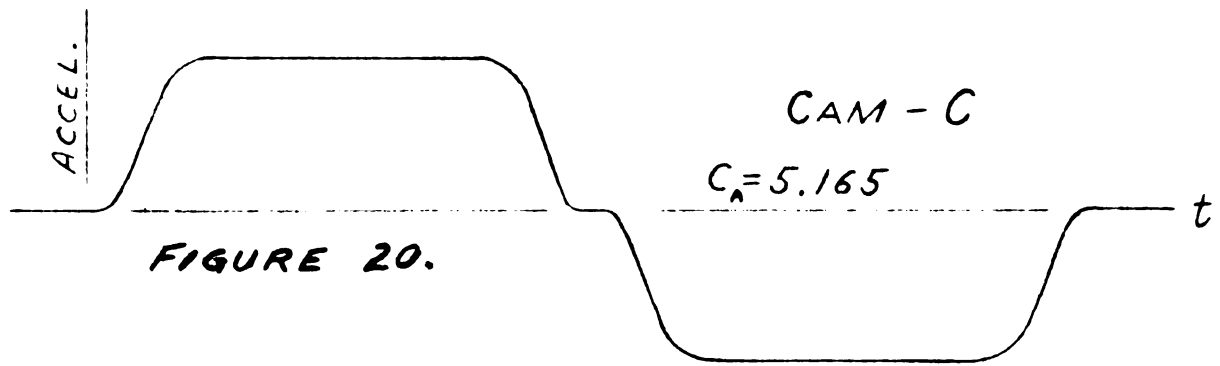




$$\begin{array}{ll}
 0 \leq t \leq .125 & \ddot{x} = .5[1 - \cos 8\pi t] \\
 .125 \leq t \leq .375 & \ddot{x} = 1.0 \\
 .375 \leq t \leq .50 & \ddot{x} = -\sin 4\pi t \\
 .50 \leq t \leq 1.0 & \ddot{x}(t) = -\ddot{x}[1-t]
 \end{array}$$



$$\begin{array}{ll}
 0 \leq t \leq .125 & \ddot{x} = .5[1 - \cos 8\pi t] \\
 .125 \leq t \leq .375 & \ddot{x} = 1.0 \\
 .375 \leq t \leq .50 & \ddot{x} = .5[1 - \cos 8\pi t] \\
 .50 \leq t \leq 1.0 & \ddot{x}(t) = -\ddot{x}[1-t]
 \end{array}$$



$$t = 0$$

$$\ddot{x} = 0$$

$$0 < t < .50$$

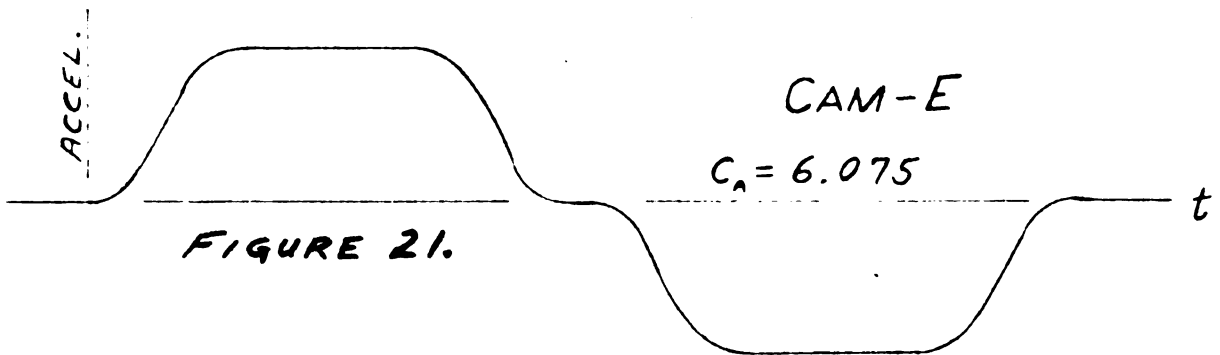
$$\ddot{x} = e^{-7.825[4t-1]^{10}}$$

$$t = .50$$

$$\ddot{x} = 0$$

$$.50 < t \leq 1.0$$

$$\ddot{x} = -\ddot{x}[1-t]$$



$$t = 0$$

$$\ddot{x} = 0$$

$$0 < t < .50$$

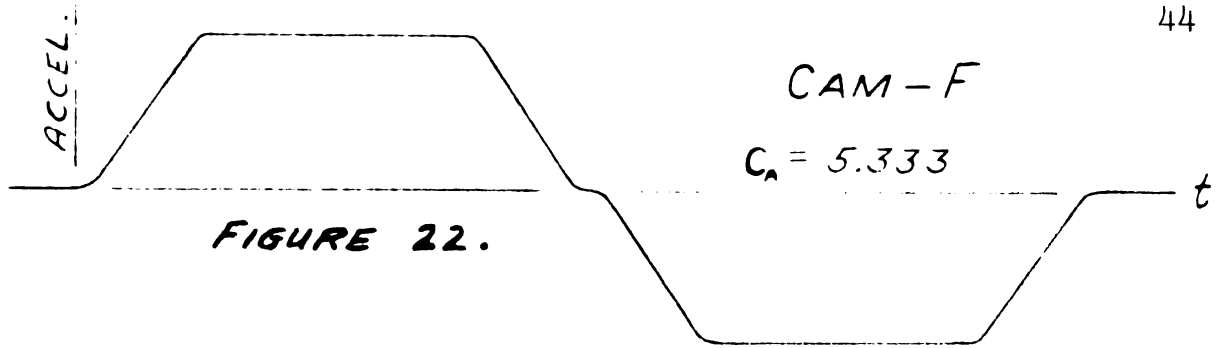
$$\ddot{x} = e^{-7.825[4t-1]^6}$$

$$t = .50$$

$$\ddot{x} = 0$$

$$.50 < t \leq 1.0$$

$$\ddot{x}(t) = -\ddot{x}[1-t]$$



$$0 \leq t \leq .0625$$

$$\ddot{x} = 1 - \frac{1}{1 + [16t]^2}$$

$$.0625 \leq t \leq .125$$

$$\ddot{x} = \frac{1}{1 + [16t - 2]^2}$$

$$.125 \leq t \leq .375$$

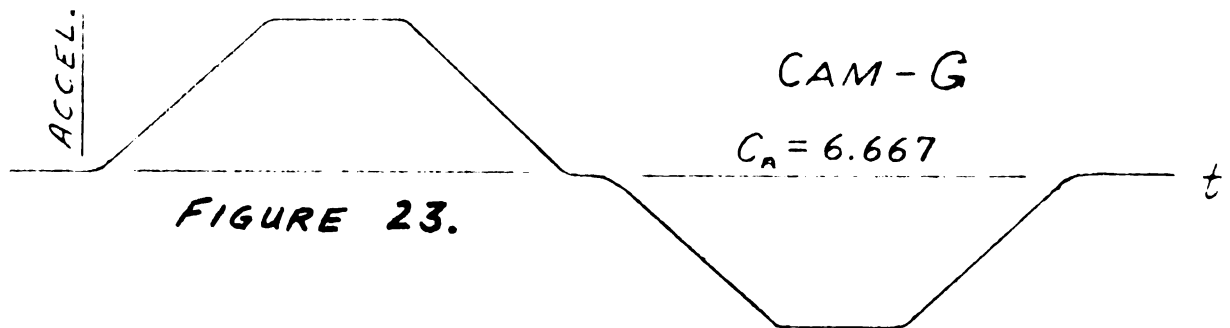
$$\ddot{x} = 1.0$$

$$.375 \leq t \leq .50$$

$$\ddot{x}(t) = \ddot{x} [.5 - t]$$

$$.50 \leq t \leq 1.0$$

$$\ddot{x}(t) = -\ddot{x} [1 - t]$$



$$0 \leq t \leq .10$$

$$\ddot{x} = 1 - \frac{1}{1 + [10t]^2}$$

$$.10 \leq t \leq .20$$

$$\ddot{x} = \frac{1}{1 + [10t - 2]^2}$$

$$.20 \leq t \leq .30$$

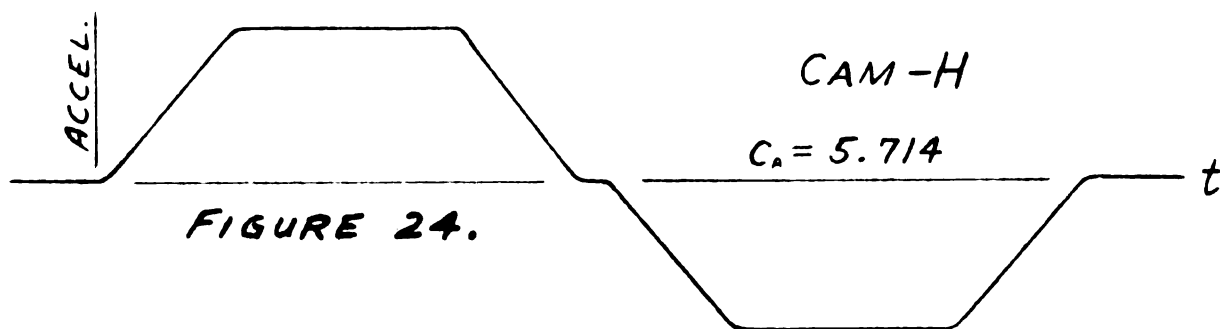
$$\ddot{x} = 1.0$$

$$.30 \leq t \leq .50$$

$$\ddot{x}(t) = \ddot{x} [.5 - t]$$

$$.50 \leq t \leq 1.0$$

$$\ddot{x}(t) = -\ddot{x} [1 - t]$$



$$0 \leq t \leq .075$$

$$\ddot{x} = 1 - \frac{1}{1 + \left[\frac{40t}{3}\right]^2}$$

$$.075 \leq t \leq .15$$

$$\ddot{x} = \frac{1}{1 + \left[\frac{40t}{3} - 2\right]^2}$$

$$.15 \leq t \leq .35$$

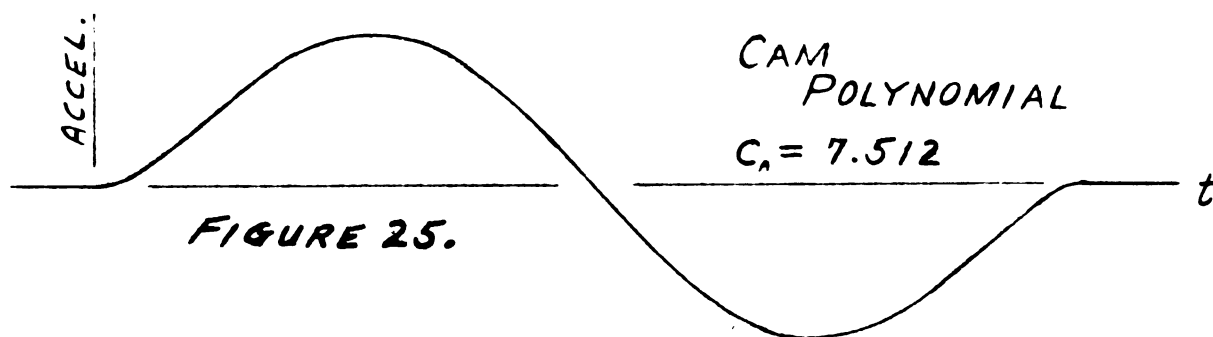
$$\ddot{x} = 1.0$$

$$.35 \leq t \leq .50$$

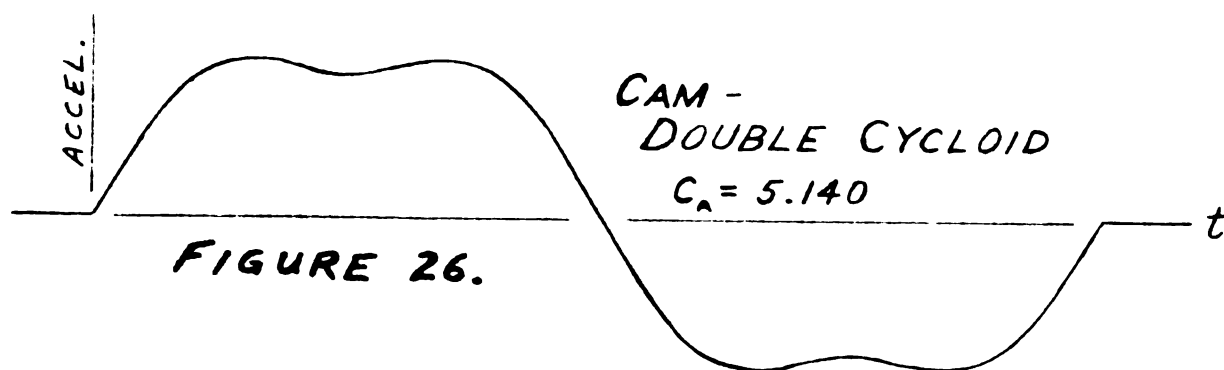
$$\ddot{x}(t) = \ddot{x} [.5 - t]$$

$$.50 \leq t \leq 1.0$$

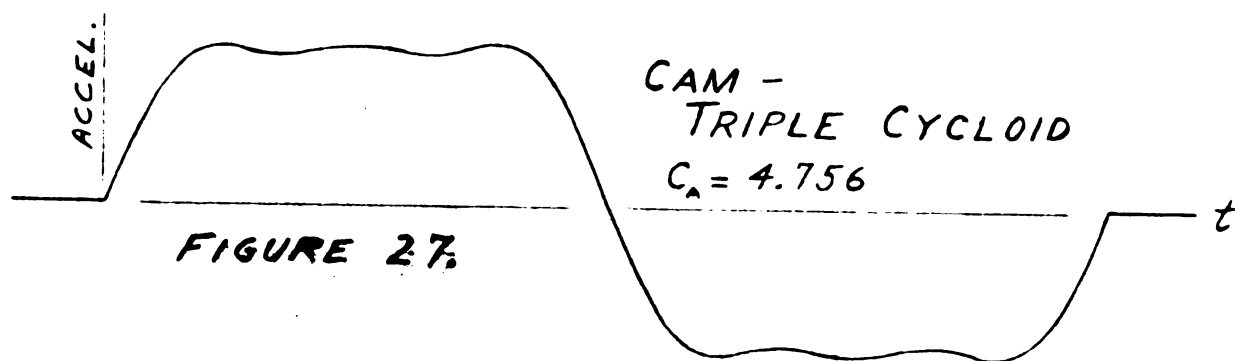
$$\ddot{x}(t) = \ddot{x} [1 - t]$$



$$\ddot{x} = -1.1181 [t - .5] [(t - .5)^2 + .25]^2$$



$$\ddot{x} = 1.1513 \sin 2\pi t + .2189 \sin 6\pi t$$



$$\ddot{x} = 1.2018 \sin 2\pi t + .3004 \sin 6\pi t + .0958 \sin 10\pi t$$

ROOM USE ONLY

Attendant dept,  
RE



MICHIGAN STATE UNIV. LIBRARIES



31293010622144